Grass root litter and soil carbon quality paradoxically control Q10 of labile and recalcitrant carbon pools in a semi-arid Inceptisol

Vikas Kumar Singhal
Avijit Ghosh
avijitghosh19892@gmail.com

Indian Grassland and Fodder Research Institute https://orcid.org/0000-0002-0556-445X

Amit K Singh
Ranjan Bhattcahryya
Yogeshwar Singh
Sourav Kumar
Deepak Ojha
Arun K Shukla

Research Article

Keywords: Carbon mineralization, Carbon-quality-temperature hypothesis, Soil organic matter quality, Grass root litter, Grasslands

Posted Date: November 5th, 2025

DOI: https://doi.org/10.21203/rs.3.rs-7771415/v1

Version of Record: A version of this preprint was published at Plant and Soil on March 4th, 2026. See the published version at https://doi.org/10.1007/s11104-026-08423-9.

Grass root litter and soil carbon quality paradoxically control Q_{10} of labile and recalcitrant carbon pools in a semi-arid Inceptisol

Running head: Soil carbon mineralization and carbon quality

Vikas Kumar Singhal[1,2], Avijit Ghosh[2,*], Amit K Singh[2], Ranjan Bhattcahryya[3], Yogeshwar Singh[1], Sourav Kumar[1,2], Deepak Ojha[2], and Arun K Shukla[2]

[1]RLBCAU, Jhansi, India, 284003

[2]ICAR-IGFRI, Jhansi, India, 284003

[3]ICAR-IARI, New Delhi, India 110012

Correspondence: Avijit Ghosh (avijit.ghosh@icar.org.in; avijitghosh19892@gmail.com)

ABSTRACT

Aim: The temperature sensitivity of labile (Q_{10L}) and recalcitrant (Q_{10R}) pools of soil organic carbon (SOC) decomposition is a critical for predicting soil carbon (C) fluxes under changing climatic conditions.

Methods: Soils under six grass covers, namely, *Cenchrus ciliaris*, *Chrysopogon fulvus*, *Panicum maximum*, *Sehima nervosum*, *Heteropogon contortus*, and *Vetiveria zizanioides* from semi-arid India were evaluated for Q_{10L} and Q_{10R} of bulk soil, macroaggregates, microaggregates, and silt+clay associated SOC. Soil fractions (from 0-20 and 21-40 cm depths) were incubated at 25, 32, and 37 °C for 100 days, and cumulative C mineralization was measured. The Q_{10L} and Q_{10R} were calculated using a two-pool decay model. The quality of root litter C and SOC was assessed through FTIR spectroscopy.

Results: Q_{10L} and Q_{10R} of microaggregate-C was significantly higher (22-64% and 22-24%, respectively) than macroaggregate-C and silt+clay-C. Among grasses, Q_{10L} and Q_{10R} values under *C.ciliaris*, *H.contortus*, and *S.nervosum* were lower than other grasses, indicating their

capability to store SOC under global warming scenarios. Q_{10L} at topsoil layer was correlated with root litter C quality and at the sub-surface soil layer, it was influenced by labile C concentration. The Q_{10R} was correlated with the recalcitrant C concentration and SOC quality in both soil layers, indicating that quality and availability of recalcitrant SOC had pivotal roles in governing Q_{10R} in restored land.

Conclusions: Soil C and litter C quality should be potentially incorporated into the biogeochemical models to better predict SOC dynamics in managed ecosystems in the context of global warming and land use changes.

Keywords: Carbon mineralization; Carbon-quality-temperature hypothesis; Soil organic matter quality; Grass root litter; Grasslands;

List of abbreviations:

C.cil: *Cenchrus ciliaris*; C.ful: *Chrysopogon fulvus*; P.max*: Panicum maximum;* S.ner*: Sehima nervosum*; H.con*: Heteropogon contortus*; V.ziz*: Vetiveria zizanioides*; URC: Unrestored control; TSL: topsoil layer; SSL: sub-surface soil layer; C_L: labile C; C_R: recalcitrant C; k_L: decay rate of labile C; k_R: decay rate of recalcitrant C; Q_{10L}: temperature sensitivity of labile C; Q_{10R}: temperature sensitivity of recalcitrant C; HI: humification index; DDI: degree of decomposition index; MA: macroaggregates; MI: microaggregates; SC: silt+clay; MI-OC: MI associated total soil organic carbon; MA-OC: MA associated total soil organic carbon; SC-OC: SC associated total soil organic carbon; DHA: dehydrogenase; GLU: β-glucosidase; PHOX: phenoloxidase; PEROX: peroxidase; Ct : Cumulative C mineralization; SOM: Soil organic matter; SOC: Soil organic carbon

Introduction

Grass-based land restoration can help to restore deteriorated soil health (Patidar et al., 2023). In restored areas, researchers have found that grasses can improve the soil microbial population (Perkins and Nowak, 2013), soil aggregation (Deng et al., 2018), and the storage of soil organic carbon (SOC) (Singhal et al., 2025). To investigate impacts of grasses on SOC storage, these aspects have often been taken into account separately (Liu et al., 2015). Although microbial carbon mineralisation determines SOC storage in soil under global warming scenarios, little research has been done to examine how grasses affect the kinetics of SOC mineralisation during vegetation restoration. In fact, because microbial activity and temperature are positively correlated, global warming would promote the microbial degradation of SOC (Crowther et al., 2016). Therefore, it is imperative to identify grasses that can enhance soil organic carbon storage following the restoration of damaged lands by counteracting soil organic carbon mineralisation. The temperature sensitivity (Q_{10}) of SOC decay, which indicates that the rate of SOC decay increases by 10 °C as the ambient temperature rises, is a major determinant of the amplitude of this stimulation (Davidson and Janssens, 2006; Friedlingstein et al., 2006). Depending on the kind of grass cover, the soil organic matter (SOM) quality of ecologically restored land varies due to presence of a variety of organic C compounds; slowly decomposable stable recalcitrant pool and quickly decomposable reactive labile pool (Davidson and Janssens, 2006). SOM consists of a variety of organic C pools with differences in physical structure, combination with soil particles and chemical recalcitrance that determines their stability in soil. Soil temperature has significant impacts on the rate of decomposition of labile and recalcitrant pools of SOM (Craine and Gelderman, 2011). In addition to temperature, the two most important factors determining Q_{10} of labile pool (Q_{10L}) and recalcitrant pools (Q_{10R}) are quality and availability these substrates (Fissore et al. 2013).

The carbon-quality-temperature (CQT) hypothesis predicts that the intrinsic Q_{10} rises with increasing recalcitrance of the SOM (Davidson and Janssens, 2006); however, apparent Q_{10} is regulated mostly by environmental conditions, such as, temperature, moisture (Liu et al., 2021). Henceforth, kinetics theory foretells that recalcitrant C will be more susceptible at high temperatures than labile C. The relationship between SOM stability and its temperature sensitivity is still up for debate, despite the fact that numerous laboratory incubation studies have empirically supported CQT theory (Bracho et al., 2016; Ghosh et al., 2020). However, other studies have found conflicting results depicting greater Q_{10} for labile soil organic carbon pool (Pang et al., 2015; Liu et al., 2021).

The impact of labile C inputs on Q_{10} has not been taken into account in many previous studies, despite the fact that substrate availability is a key driver of Q_{10} (Xu et al., 2014). Although breakdown of litter is a major source of labile C substrates in soil, the effect of litter C quality on Q_{10} has not been taken into account in previous studies. Ironically, it is anticipated that labile C inputs from decomposing roots would affect labile C mineralisation while also influencing the breakdown of resistant C. Further research is required to monitor the impact of root litter on SOC quality on Q_{10L} and Q_{10R} to understand their impact on carbon sequestration (Lavallee et al., 2020).

Root litter inputs also make the carbon mineralization kinetics more complicated by incorporating new organic materials. The quantity of root litter, its ratios of labile to recalcitrant compounds, affect microbial activity and enzyme production thus regulating the rate of decomposition of both labile and recalcitrant SOC pools. Also, the proportionality between the availability of the substrate and the quality of the substrate can change over time as litter subsides. Right after litter addition, substrate availability would most probably take centre stage in the responses of the microbes, but later periods may be due to substrate quality and recalcitrance. The physical protection of SOC that is being mediated by the soil aggregation

and organo-mineral associations could further interplay with the chemical composition and microbial process to establish the effective temperature sensitivity of each carbon fraction. Although there have been advances in the knowledge of SOC decomposition, there is a critical gap between availability of substrates, quality of substrates and SOC fraction-specific Q_{10} responses in realistic litter input conditions. The process of decoupling these interactions is crucial to the proper prediction of carbon cycle feedbacks in a warming climate, especially in ecosystems where root-derived contributions make up a large proportion of SOC. Furthermore, variable chemical recalcitrance, physical protection, and enzymatic breakdown processes of SOM could lead to variations in Q_{10L} and Q_{10R} of SOM considerably. Regretfully, Q_{10L} and Q_{10R} of SOM has not been independently measured in many investigations.

The Q_{10} of SOC varies largely in grasslands. In Chinese grasslands, the Q_{10} values ranged from 1.03 to 8.13 (mean 2.60±0.08). Moreover, the Q_{10} values varied largely within and among grassland types and soil temperature measurement depths (Feng et al., 2018). Among grassland types, the highest Q_{10} occurred in alpine grasslands. They suggested that the combined factors of soil temperature and moisture would better predict soil respiration in arid and semi-arid regions, and implied that alpine grasslands in China might release more carbon dioxide to the atmosphere under climate warming. However, grass type-controlled soil carbon decomposition processes in snowy mountains region of NSW, Australia, with potential implications for feedbacks under warming conditions—especially via increased sensitivity of recalcitrant carbon (Jenkins and Adams, 2011). A global review by Wang and Fang (2009) revealed that the Q_{10} values of grassland varied from 0.9 to 4.6. The modal Q_{10} values ranged from 1.5 to 2.0 with an overall mean of 2.13. The mean Q_{10} values were 2.23 and 1.94 in temperate and tropical grasslands, respectively. They also described that root and soil respiration were majorly responsible for the variability of the Q_{10} value.

We conducted a laboratory incubation under three temperatures (25, 32, and 37 °C) to monitor CO_2 respiration from bulk soil, macroaggregates, microaggregates, and silt+clay fractions of six grass covers in restored semi-arid lands of India, and quantified Q_{10L} and Q_{10R}. We further examined the simultaneous effects of root litter C quality and SOM quality on these temperature sensitivities. In semi-arid ecologically restored degraded land, our primary targets were to: 1) evaluate the effects of different grass covers on Q_{10L} and Q_{10R} and 2) determine whether the CQT hypothesis applies to ecologically restored degraded lands (which originally had a low C content) with a constant supply of labile C from root litter. We posit that: 1) labile substrate availability would increase the Q_{10L} due to the cancelling effect according to Michaelis–Menten kinetics, whereas, Q_{10R} will be enhanced by the SOM recalcitrance; 2) after root litter decomposition, the effect of substrate availability on Q_{10L} and Q_{10R} would be more important than that of substrate quality; and 3) the changes in Q_{10L} and Q_{10R} would be differently influenced by root litter C and soil C quality due to their variable chemical recalcitrance, physical protection, and enzymatic decomposition mechanisms (Fig. 1a and 1b).

Materials and methods

Experimental strategies

The experimental site was located at a degraded landscape in Jhansi, Uttar Pradesh, India (Fig. 1). The primary drivers of degradation were soil erosion, poor soil fertility, low organic matter content, and low rainfall. The properties of soil prior to restoration were measured during Pre Monsson season of 2015. The soil properties before restoration and climatic variables during the study period are tabulated (Table S1). The URC had low (1.00 g kg^{-1}), poor soil available phosphorus (P; 9.1 kg ha^{-1}), available nitrogen (N; 182 kg ha^{-1}), and available potassium (K; 252 kg ha^{-1}). The URC had high soil erosion (>10 Mg ha^{-1}). The restoration programme was introduced in rainy season of 2015 (July 2015) and is continuing to date. The high temperature during summer, erratic monsoon, high aridity index, and insufficient profile moisture

categorize the region as semi-arid. From the start of the restoration programme, an unrestored fallow control land (URC) was maintained with identical slope, topography, texture, and parent material for future assessment of possible changes in soil properties. Three replicated strips for each grass were identified after randomization (Fig. 1c). Barren land was converted to grasslands with six tropical perennial grasses, namely *Cenchrus ciliaris* (C.cil), *Chrysopogon fulvus* (C.ful), *Panicum maximum* (P.max), *Sehima nervosum* (S.ner), *Heteropogon contortus* (H.con), and *Vetiveria zizanioides* (V.ziz). During mid-July, 2015, seedlings of each grass was planted at a rate of 10 seedlings m^{-2}. For every grass, a model plot (10 m × 15 m) was created. They were watered two to three times throughout the first two years to ensure a consistent plant population of each grass for improved establishment. The grasses were then acclimated to surviving solely on rainwater, and no irrigation was used. The restored land was not allowed for grazing. Every year, during mid-November, the aboveground biomass of grasses is taken, allowing the tussock to flourish throughout the upcoming monsoon season. The triplicates of 2 m × 2 m sub-plots, randomly distributed in the model 10 m × 15 m plots, were identified for measuring pasture productivity and soil properties. The biomass productivity of grasses in field was estimated in three replicates of uniform area of 2 m × 2 m. The soil of the whole experimental area had similar SOC, texture, slope, pH, water holding capacity, and nutrient availability.

Measurements of above ground biomass, root biomass, and root C quality

Samples of plant and soil were collected after harvesting of grasses from regions with consistent population density of grasses and soil physiography. For every grass, three sampling points were spotted within a model plot. Soil samples were collected using a core from top (TSL: 0–20 cm) and sub-surface (SSL: 21-30 cm) layers for restored area and URC. These soil samples were quickly taken to the laboratory and divided into two splits: one was stored at 4°C to evaluate microbiological characteristics, while the other was allowed to air dry and was used

to examine physical and chemical data. The grasses were acquired, tagged, and kept in paper bags before being dried in an oven (65 ± 2°C) until they reached a constant weight. The dry mass was determined and reported in as dry matter production (g m^{-2}). The dead roots were collected using cores from 0-20 and 21-40 cm soil layers and were washed with water and ethyl alcohol and their functional groups of roots were studied using a FTIR spectrometer (Bruker; Alpha II). The abundance of carboxylate and polysaccharides were detected by the peak absorbance at 1410 and 1050 cm^{-1}, respectively. Similarly, the abundance of aromatic + phenolic (by peak absorbance at 1520 and 1610 cm^{-1}) and aliphatic (2983 and 2921 cm^{-1}) compounds were also identified using FTIR spectra. The morphological parameters of roots were studied using a root analyzer.

Root decomposition kinetics

Roots were collected by excavating one grass tussock for each grass. The soil burying approach was also used to determine the rate of root degradation. Air dried roots of every grass (100 g) was placed in a paper bag and covered with soil. To retrieve the undecomposed root, each paper bag was put into a 30 cm × 15 cm nylon-mesh litter bag. Total 10 litter bags for each grass (each bag containing 100 g root of a grass) was placed in soil. On each sampling day (i.e. 30^{th}, 60^{th}, 90^{th}, 120^{th}, and 180^{th} days after burial (DAB)), two samples of each grass were taken out (Magh et al., 2024). The dry root mass was noted on each sampling date. The decay kinetic of root was assessed with an exponential equation:

$$Mt = M0(1 - \exp(-rt)) \dots (1)$$

where, Mt is the mass of decomposed roots after t DAB, M0 is the mass of potentially decomposable root, r is decomposition of root (RDR)

Separation of soil aggregate and estimation of soil organic carbon

Aggregates from bulk soil (passed through 4.75 mm sieve) were separated using a yoder apparatus in wet sieving and classified as macroaggregate fraction (MA; >250-4750 μm), microaggregate fraction (MI; 53–250 μm), and silt+clay (SC; <53 μm) (Six et al., 2000). Total SOC concentrations in bulk soil, MA, MI, and SC were measured through dry combustion-oxidation method using an enviro TOC analyzer (enviro TOC analyzer; ELEMENTAR). Labile and recalcitrant pools of SOM were estimated for bulk soil, MA, MI, and SC (Rovira and Vallejo, 2002). In first step, 500 g samples were hydrolyzed with 20 ml of H_2SO_4 (2.5 M) at 105 °C for half an hour. The hydrolysed substances were collected through centrifugation. In second step, the remaining part was cleansed with ion free water and oven dried at 40 °C. Thereafter, the samples were shaken for overnight after adding 2 ml of H_2SO_4 (13M). The strength of acid was diluted to 1M by adding water. The samples were then hydrolyzed for 3 h at 105 °C. The hydrolysed substances were collected through centrifugation. The hydrolysed substances collected in two steps constituted the labile pool of SOM. The residue was cleansed again, oven-dried at 65 °C. It constituted the recalcitrant pool of SOM (Rovira and Vallejo, 2002). The labile and recalcitrant pools were analysed for labile C and recalcitrant C, respectively, using an enviro TOC analyzer.

Furthermore, absolute activities of extracellular soil enzymes in bulk soils, namely, dehydrogenase (DHA), glucosidase (GLU), phenoloxidase (PHOX), and peroxidase (PEROX) were assessed using substrate-based incubation methods, where, triphenyl tetrazolium chloride, p-nitrophenol glucoside, and 2,2′-azinobis(3-ethylbenzothiazoline-6-sulfonic acid) were used as substrate (Dick, 2011). Specific activities of soil enzymes were estimated by dividing absolute activities of extracellular soil enzymes with their respective concentration of SOC.

Measurements of C mineralization kinetics and temperature sensitivity

Five hundred grams of sieved and air-dried samples from bulk soil, MA, MI, and SC was taken into 100 mL glass jar. The samples were subjected to preincubation at 50% water holding

capacity at 27 °C for 14 days to overcome the impact of rewetting and sieving on microbial respiration (Zacháry et al., 2018). The preincubated soils from bulk soils, MA, MI, and SC were divided into three parts for incubation at three temperatures, i.e. 25, 32, and 37 °C. Three replicates of soil (each weighing 50 g) from bulk soils, MA, MI, and SC were taken in a 250 mL glass jar for incubation at a specific temperature. Three blank sample without soil was used for the whole incubation experiment at each specific temperature. The samples were kept in a dark incubator at specified temperatures for 100 days at 70% WHC to avoid disintegration of soil aggregates during handling (Frøseth and Bleken, 2015). The CO_2 was trapped in glass vials containing 12 ml of 1 M NaOH, placed in the air-tight incubation jars. The NaOH traps were replaced on days 2, 7, 14, 21, 49, 70 and 100. The amount of CO_2 evolved was measured by titrating the NaOH with 1 M HCl in the presence of $BaCl_2$ (Anderson, 1982). The cumulative carbon production was fitted to the following two-pool model

$$C_t = C_L(1 - e^{-k_L \times t}) + C_R(1 - e^{-k_R \times t}) \dots (2)$$

C_t is mineralized carbon during t days of incubation. C_L is labile C pool, k_L is labile C pool mineralization constant, C_R is recalcitrant C pool, k_R is recalcitrant C pool mineralization constant.

A non-linear exponential equation was employed to relate k_L and k_R with temperatures (Eqs. 3 and 5) and the Q_{10L} and Q_{10R} were estimated by Eqs. 4 and 6 (Fierer et al., 2006; Ghosh et al., 2020).

$$k_L = M_{0L}e^{pt} \dots (3)$$

$$Q_{10L} = e^{10p} \dots (4)$$

$$k_R = M_{0R}e^{qt} \dots (5)$$

$$Q_{10R} = e^{10q} \dots (6)$$

240 M_{0L} and M_{0R} signifies the mineralization rate of C_L and C_R at 0 °C temperature, p and q are
241 temperature coefficients for C_L and C_R, respectively. Q_{10L} and Q_{10R} are temperature sensitivity
242 for C_L and C_R, respectively.

243 **Estimation of soil organic matter quality**

244 The air-dried samples from bulk soils, MA, MI, and SC were taken to a 100 mL plastic
245 centrifuge tube. Hydrogen fluoride (HF) solution (10% v/v) was added to the soil at a ratio soil
246 to solution of 1:10. The resultant mixed solution was shaken for an hour and centrifuged for
247 10 min (3000 rpm), and the residue was collected. Successively, the same procedure was
248 repeated with residual part of sample for eight times with different period of shaking (4 repeats
249 with 1 h shaking, 3 repeats with 12 h shaking, and 1 repeat with 24 h shaking, serially). At last,
250 the residual sample was washed with ion-free water for 6 times to discard any residual HF in
251 the sample adding 50 mL water, followed by 10 min shaking and centrifugation (at 3000 rpm)
252 for 10 min. The purified samples were oven-dried at 45 °C, ground through a 250µ sieve, and
253 stored in a polythene bag for FTIR spectroscopy. The SOM from bulk soils, MA, MI, and SC
254 were spectrally characterised with a scan range of 4000-400 cm^{-1} and a resolution of 4 cm^{-1}. 50
255 scans were performed for each sample. The OPUS 2023 was used for processing spectral data
256 to correct the baseline, smoothing, and normalisation. The peak intensity (by height) was
257 recorded to assess the magnitude of infrared absorption of the selected peaks. The SOM was
258 characterized by estimating the following quality parameters using spectral absorption (Obeng
259 et al., 2023).

260 $$\text{Humification index-a (HI)} = \frac{\text{CC (Absorption at 1410 } cm^{-1})}{\text{PC (Absorption at 1050 } cm^{-1})} \dots (7)$$

261 Where CC is carboxylate compounds and PC is polysaccharide compounds

262 $$\text{Degree of decomposition index (DDI)} = \frac{\text{HC (Absorption at 1720 } cm^{-1})}{\text{ALC (Absorption 2983 + 2921 } cm^{-1})} \dots (8)$$

263 Where HC represents hydrophilic compounds and ALC represents aliphatic compounds.

264 $$\text{Aromaticity index} = \frac{\text{ARC (Absorption at } 1620 + 1520\ cm^{-1})}{\text{ALC (Absorption } 2983 + 2921\ cm^{-1})} \ldots (9)$$

265 Where, ARC represents aromatic compounds.

266 **Statistical analysis**

267 The data was analyzed for variance analysis using one-way ANOVA to test for variations across
268 the grasses. We assume that a) soils are randomly sampled and independently chosen from the
269 populations; b) variances of each sample are equal; c) the residuals are normally distributed.
270 The Tukey test was conducted at $P < 0.05$ to differentiate the means. The Pearson correlation
271 was used to interpret the interrelations among the variables.

272 We used a path model (i.e., structural equation model) depicting impact of labile and
273 recalcitrant C pools (C_L and C_R), soil organic matter quality, and root litter C quality on
274 temperature sensitivity of labile and recalcitrant C pools (Q_{10L} and Q_{10R}) at top and sub-surface
275 soil layers, respectively. The suitability of the model was verified by $\chi 2$-test, goodness of fit
276 (GFI) index, and root mean squared error of approximation (RMSEA). Favourable model fits
277 were indicated by no significant difference on the $\chi 2$-test ($P > 0.05$), high GFI (> 0.60), and
278 low RMSEA (< 0.075).

279 **Results**

280 **Above and below ground biomass production and bulk soil carbon concentration**

281 Among the grasses, P.max had the highest above ground biomass yield, followed by C.ful,
282 C.cil, and H.con (Table S2). However, the root biomass was significantly higher for C.cil. The
283 root biomass of P.max, C.ful, and H.con were similar. The decay rates of roots of C.cil, S.ner,
284 and H.con were significantly higher than other grasses. The SOC concentrations in bulk soils

were the highest under C.cil in both soil layers. Despite, P.max having higher above ground biomass, C.cil had greater SOC than P.max at the TSL and SSL (Table S2). The H.con and S.ner had significantly higher ($p<0.05$) SOC at the TSL and SSL than V.ziz. At TSL, bulk soil C_L values under C.cil and S.ner were significantly higher ($p<0.05$) than P.max, whereas, at the SSL, C.cil had only significantly greater bulk soil C_L than P.max (Table 1). The C_L was significantly higher under all grasses over URC. The bulk soil C_R values under C.cil and S.ner were significantly higher ($p<0.05$) at TSL and SSL than P.max.

Soil aggregation, aggregate associated C, and carbon pools

The mass of MA and MI increased under all grasses as compared to URC (Fig. 2A). However, in the TSL, the mass of MA was ~14-38% greater under different grasses and that of MI was ~20-55% higher under those grasses over URC. In the SSL, the mass of MA increased by ~11-54% under those grasses over URC. The mass of SC declined by 1.62-2.23 times at the TSL and 1.50-2.31 times at the SSL in restored land compared to URC.

The C.cil, H.con, and S.ner had significantly higher ($p<0.05$) MA-OC at the TSL and SSL compared to P.max (Fig. 2B). The C.cil and S.ner also had significantly greater ($p<0.05$) MI-OC at the TSL compared to P.max. The C.cil, H.con, and S.ner had significantly greater ($p<0.05$) MI-OC at the SSL compared to P.max. These three grasses resulted in significantly greater ($p<0.05$) SC-OC at the TSL and SSL compared to P.max. The mean (of six grass types) MI-OC values were ~26-55 and 11-16% greater than the mean MA-OC and SC-OC, respectively (Fig. 2B). The MA-C_L values under C.cil, H.con, and S.ner were also significantly higher ($p<0.05$) than P.max at the TSL. Although, thethe MA-C_L values were significantly higher ($p<0.05$) under C.cil and S.ner than P.max, at the SSL; P.max and H.con had similar MA-C_L at the SSL (Table 1). Contradictorily, the MI-C_L under C.cil was significantly higher ($p<0.05$) than P.max; H.con and S.ner had identical MI-C_L to P.max at the TSL. However, the MI-C_L under C.cil, H.con, and S.ner were significantly higher ($p<0.05$) than P.max at SSL. The

SC-C_L followed the similar trends to MA-C_L at the TSL. The MA-C_L, MI-C_L, and SC-C_L were significantly lower under C.ful and V.ziz than other grasses, although they had greater MA-C_L, MI-C_L, and SC-C_L than URC at the TSL and SSL (Table 1). The MA-C_R values under C.cil, H.con, and S.ner were also significantly higher ($p<0.05$) at the TSL and SSL than P.max. The MI-C_R and SC-C_R flowed the similar trends. The MA-C_R, MI-C_R, and SC-C_R values were significantly lower under C.ful and V.ziz than other grasses, although they had greater MA-C_R, MI-C_R, and SC-C_R values than URC at the TSL and SSL (Table 1).

Cumulative C mineralization

The cumulative carbon mineralization (C_t) values of bulk soil, MA, MI, and SC were significantly higher under P.max than C.cil, H.con, and S.ner at all temperatures and soil layers (Fig. 3a-h; Fig. S1). However, the C_t values of bulk soil, MA, MI, and SC at TSL were significantly higher than SSL. For bulk soils, C_t values at 32 and 37 °C were similar to that at 25 °C. For MA, MI, and SC, C_t values at 32 and 37 °C were significantly ($p<0.05$) higher than that at 25 °C, respectively. Overall, mean (of six grass types) C_t values of MA were ~6-20% lower than that of bulk soil. However, mean (of six grass types) C_t of MI were ~16-30% greater than that of MA, whereas, mean (of six grass types) C_t values of SC were ~29-36% lower than that of MA (Fig. 3a-h). The proportion of C_t from bulk soils and aggregate fractions at both soil layers were higher for P.max and C.ful compared to other grasses (Fig. S1). The proportion of C_t were significantly higher for bulk soils than aggregates. Among the aggregates, the proportion of C_t for MA was significantly greater than that of MI and SC at all soil layers.

C mineralization kinetics

The decay rates of labile and recalcitrant C in bulk soil, MA, MI, and SC were significantly lower under all grass cover compared to URC (Table 2). Among the grasses, V.ziz had higher k_L and k_R than other grasses for bulk soil and aggregates. The k_L values under C.cil, H.con, and

S.ner were significantly ($p<0.05$) lower than V.ziz in bulk soils, MA, MI, and SC at all temperatures and soil layers. However, at the SSL, the bulk soil k_L data under C.cil and S.ner were significantly lower than V.ziz at all temperatures, whereas, k_L of MA, MI, and SC under C.cil, H.con, and S.ner were significantly lower than V.ziz. The k_R values under C.cil, H.con, and S.ner were significantly ($p<0.05$) lower than V.ziz in bulk soils, MA, MI, and SC at all temperatures and soil layers. At the SSL, the bulk soil k_R values under C.cil, H.con, and S.ner were similar; however, the k_R values of MA, MI, and SC under C.cil was significantly lower than that of S.ner and H.con at all temperatures (Table 2).

The mean (of six grass types) k_L at 32 and 37 °C increased by 1.07 – 3.16 times at TSL and 1.02 – 2.04 times in the SSL over that at 25 °C across soil fractions. The mean (of six grass types) k_R at 32 and 37 °C increased by 1.09 – 1.47 times at TSL and 1.11 – 1.36 times at the SSL over that at 25 °C across soil fractions. The mean (of six grass types) k_L values for bulk soils and MA at SSL were significantly higher than that at the TSL at all temperatures. Contrarily, the mean (of six grass types) k_R at the TSL was significantly higher than that at the SSL for all soil fractions at all temperatures (Table 2).

Temperature sensitivity

The temperature sensitivity of labile C (Q_{10L}) was significantly influenced by grass type. For bulk soil, the Q_{10L} values under C.cil, H.con, and S.ner were significantly ($p<0.05$) lower at the TSL and SSL than V.ziz (Table 3). For MA, MI, and SC, the Q_{10L} under C.cil and H.con were significantly ($p<0.05$) lower than V.ziz at the TSL and SSL than C.ful. The temperature sensitivity data of recalcitrant C (Q_{10R}) of MA, MI, and SC under C.cil, H.con, and S.ner were significantly ($p<0.05$) lower at the TSL and SSL than V.ziz. The Q_{10L} and Q_{10R} of bulk soils were similar at the TSL and SSL. The means (of six grass types) Q_{10L} and Q_{10} values for MA, MI, and SC at the TSL were significantly ($p<0.05$) higher than SSL, respectively. The means

(of six grass types) Q_{10L} and Q_{10} values for MA, MI, and SC at the TSL and SSL were significantly ($p<0.05$) higher than those of bulk soils (Table 3).

Activities of soil enzymes

The activities of DHA, GLU, PHOX, and PEROX were significantly higher under C.cil, H.con and S.ner compared to C.ful, P.max, and V.ziz at both soil layers (Fig. 4a). However, specific activities of these enzymes were significantly lower under C.cil, H.con, and S.ner than P.max at both soil layers (Fig. 4b).

The root litter carbon and soil carbon quality

The abundance of carboxylate groups was significantly higher in roots of C.cil and S.ner over other grasses. The polysaccharide compounds were more profound in roots of C.cil, H.con, and S.ner over other grasses. The distribution of aromatic+phenolic compounds was higher under roots of C.cil and S.ner over other grasses. The abundance of aliphatic compounds was higher in roots of C.cil, P.max, and H.con over other grasses (Fig. 5a-b). The HI values of SOC in bulk soils, MA, Mi, and SC were significantly higher under C.cil, H.con, and S.ner than other grasses at both soil layers (Table 4; Fig. S2 and S3). The HI(a) values of SOM in MA, MI, and SC were significantly ($p<0.05$) higher than bulk soils at the TSL. The aromaticity of SOM in MA, MI, and SC was significantly ($p<0.05$) greater than bulk soils at the TSL. Similar results stand true at SSL also (Table 4; Fig. S2 and S3).

Impact of root litter carbon and soil carbon quality on Q_{10}

At the TSL, the Q_{10L} values of bulk soils, MA, and MI were positively impacted by root C quality parameters, such as, carboxylate and polysaccharide content, whereas, the Q_{10L} of SC was positively impacted by aliphatic groups in roots (Table 5). The Q_{10L} of bulk soils, MA, MI, and SC was impacted by the abundance of aromatic+phenolic compounds in roots.

Interestingly, at the SSL, the root C quality had no significant influence on Q_{10L} and Q_{10R}. The Q_{10L} of bulk soils was directly related to C_L concentration and inversely related to aromaticity at the TSL, whereas, the Q_{10L} data of MA and MI were influenced by aromaticity of SOC only. However, the Q_{10L} of SC was impacted by its C_L at the TSL (Table 5). The Q_{10R} data of bulk soils, MA, MI, and SC were impacted by humification indices, aromaticity (except SC), and concentration of C_R at the TSL. At the SSL, the Q_{10L} values of bulk soils, MA, SC, and MI were not impacted by root C quality parameters. The Q_{10L} values of bulk soils, MA, SC, and MI were positively impacted by C_L and inversely related to aromaticity (except SC). The Q_{10R} data of bulk soils, MA, MI, and SC were influenced by humification indices, aromaticity (except SC), and concentration of C_R at SSL. Overall, the Q_{10L} values of bulk soils, MA, and MI were influenced by root C quality, whereas, Q_{10R} of bulk soils, MA, MI, and SC were significantly influenced by root C quality, soil C quality and quantity at the TSL. At the SSL, Q_{10L} values of bulk soils, MA, MI, and SC were impacted by C_L quantity only and Q_{10R} of bulk soils, MA, MI, and SC were impacted by C_R quality and quantity (Table 5).

Discussion

Grasses for improving soil aggregation and C pools

The grasses had a major effect on the aggregate size distribution. The considerable decline in mass of MI (aggregates < 250 μm) and significant increase in mass of MA after grass cover establishment implied that the MI transformed to MA and consequently stabilized the soil structure (Fig. 2A). In this study, the greater mass of MI in URC indicated its further deterioration than grass cover (Zhu et al., 2017). Furthermore, the results revealed that there were a greater mass of macroaggregates for the C.cil, H.con, and S.ner compared with URC, which corresponded with the results of the earlier study (Zhong et al., 2021).

The C_L is vital for soil aggregation. This study also found the significant correlation of C_L with MA ($R^2 = 0.73$; $p<0.05$). The linkage of C_L to soil minerals or MI might be responsible for MA

formation (Bucka et al., 2019). Additionally, the root decomposition products of different grasses enacted as active binding agents. Adsorption of organic decomposition products (such as polysaccharides; organic acids, etc) to mineral surfaces might happen through hydrogen bonding, van der Waals interaction, and long-range electrostatic interaction (Bucka et al., 2019). Additionally, the occurrence of hydroxy group, methylene C-H asymmetric stretch, open-chain azo group, open chain imino group, cyclohexane ring, and secondary amine with CN stretch at the root surface of C.cil, H.con, and S.ner (Fig. 5) could assist in ligand formation to stabilize MA (Sarkar et al., 2018) (Fig. 2A and 2B). The greater stability of aggregates of S.ner and C.cil might be linked to their corresponding enzyme activities, root decay rates, and C_L contents (Fig. 4A and 4B; Tables 2 and 3). Of late, researchers have also revealed that improvements in soil structural stability are connected with gains in SOC throughout the plant establishment phase because SOC functions as a cementing and consolidating agent to enhance soil aggregate synthesis and stability (Peng et al., 2023).

Among the soil layers, the SOC under all grasses had a decreasing trend at the SSL (Table 1). The reason could be that the majority of root biomass was accumulated at the TSL, the greater microbial activity facilitating decomposition organic matter and promoting C at the TSL over SSL (Xiao et al., 2020). The SOC content varied with the decrease in the soil aggregate size and supports the findings of Fang et al. (2015). This might have occurred due to short span of restoration and it might have restricted the transfer of SOC from the MI and SC to the MA.

This could have happened as a result of the study's inadequate vegetation restoration period and the failure to transfer the SOC from the MI and SC into the MA. This is due to the fact that SOC eventually moves to the macro aggregates after first accumulating in the SC and MI (Yang et al., 2024). The influences of MI grew and the SOC of MA progressively declined as soil depth increased. This suggests that the deeper is the soil layer, the stronger are the impacts of MI on SOC and the weaker the physical effects of MA on SOC. Zhong et al. (2021)

hypothesised that a lower degree of stable MA formation is caused by a lower soil clay content linked to a relatively small aggregate size (Hontoria et al., 2016). Previous research has clearly shown that, along with this portion of the soil nutrients, MAs are readily lost from deteriorated soil due to wind erosion and runoff (Qiu et al., 2015). As a result, SOC in recovered regions is vulnerable to loss. This might be the cause of MA's lower SOC compared with MI. In particular, due to their considerably larger root biomass and root degradation rate, C.ful, H.con, and S.ner exhibited higher SOC content than other grasses (Singhal et al., 2025).

Grasses control over C mineralization kinetics

The greater C_t from bulk soil and macroaggregate of URC was due to lower protection of SOC and the greater proportion of labile C in URC (Ma et al., 2019). The greater C_t under P.max at all temperatures and soil layers compared to other grasses was due to poor soil aggregation (Fig. 2A and 2B), higher specific activities of enzymes (Fig. 4A and 4B), and lower humification ratio (Table 4) under P.max (Wagai et al., 2013). The greater Ct at the TSL than SSL could possibly be linked to higher substrate availability and greater activities of soil enzymes (Ghosh et al., 2025). The non-significant impact of temperature rise on bulk soil Ct could be related to greater C_L to SOC ratio than C_R to SOC at both soil layers. The higher proportions of C_L ensured its mineralization at low temperature; with increase in temperature substrate deficiency in bulk soils restricted its Ct, hence a non-significant significant impact of temperature was observed (Canisares et al., 2023). Despite this, the significant increase in Ct of MA, MI, and SC with increase in temperatures could be related to greater proportions of MA-C_R, MI-C_R, SC-C_R than bulk soil C_R (Table 1) and also secondary supply of labile compounds by decomposition of recalcitrant substrates (Larionova et al., 2007). The solubility and reactivity of recalcitrant substrates and substrate affinity of enzymes increased with increasing temperatures, leading to a significant rise in Ct at higher temperature (Ma et al., 2019). The lower Ct in aggregates than bulk soils could be due to higher humification ratio,

456 lower DDI (Table 4), lower proportion of C_L in aggregates than bulk soil as well as physico-
457 chemical protection of C_L and C_R within aggregates. The lowest Ct in SC could be due to strong
458 chemical bonding of C_L and C_R with clay and higher humification ratio than that in MA, MI,
459 and bulk soils. Over the course of 100 days of incubation at SSL, mineralisation caused the
460 loss of approximately 62-79% of the potentially mineralised C at 25 °C. Therefore, depletion
461 of potentially mineralizable C resulted in a nonsignificant rise in carbon mineralisation at SSL
462 even after raising the incubation temperature to 37 °C from 32 °C. Oligotrophic bacteria, which
463 are better suited to mineralise the residual, more complex organic substances (cellulose, lignin)
464 of the roots, outcompeted copiotrophs when the majority of the potentially mineralizable C was
465 depleted (Potthast et al., 2010). Furthermore, there was a nonsignificant rise in carbon
466 mineralisation at the SSL layer due to the reduced amount of labile C not being able to supply
467 enough substrate for mineralisation at 35 °C.

468 The greater k_L and k_R under V.ziz at all temperatures and soil layers over other grasses could
469 be related to poor soil aggregation, low humification ratio, and higher specific activities of
470 enzymes (Wagai et al., 2013). On the other hand, lower k_L and k_R under C.cil, S.ner, and H.con
471 at all temperatures and soil layers could be associated with improved soil aggregation (Fig. 2A)
472 and lower specific activities of enzymes (Fig. 4B). The non-significant impact of temperature
473 rise on k_L and k_R of bulk soil could be related to similar proportion of Ct to SOC (~22%) at all
474 temperatures. Despite this, the significant increase in k_L and k_R of MA, MI, and SC at higher
475 temperatures could be related to increasing Ct at higher temperatures. The greater solubility
476 and reactivity of labile and recalcitrant compounds as well as substrate affinity of enzymes
477 within aggregates at higher temperatures might have caused significant rises in k_L and k_R at
478 higher temperatures. The greater k_L at the TSL than SSL in bulk soil and aggregates could be
479 related to greater C_L and activities of DHA and GLU (Fig. 2A) in addition to the influence of
480 root C quality (Canisares et al., 2023). The greater k_R in bulk soils and aggregates at the TSL
481 than SSL could be related to greater C_R and activities of PHOX and PEROX (Fig. 2A) in

addition to the influence of soil C quality. The lower k_L in aggregates compared with bulk soils could be related to higher humification ratio, lower DDI (Table 4), lower proportion of C_L in aggregates than bulk soils as well as physico-chemical protection of C_L within aggregates (Fig. 2A). The greater k_R in aggregates than bulk soils at the TSL could be related to greater proportion of C_R in aggregates than bulk soils. The decay rate of SOC in the subsurface layer increased significantly over the surface layer due to the higher specific activities of the enzymes, which resulted in the degradation of a greater quantity of SOC for the same enzyme activity.

Grasses for governing Q_{10} of semi-arid restored land

The greater Q_{10L} in bulk soils, MA, MI, and SC of V.ziz, C.ful, and P.max than other grasses could be due to poor soil aggregation (Ghosh et al., 2020), greater specific activities of DHA and GLU, and lower humification ratio (Wagai et al., 2013). The lower mean Q_{10L} in MA over MI and SC in restored land could possibly be linked with greater physical protection of C within MA due to their greater mass and lower specific surface area. Initially, the degraded area was SOC-limited (Table S1). In accordance to our first hypothesis, the highest Q_{10L} in MI could be related to the highest proportion of C_L in MI over other aggregates after restoration, ensuring substrate availability at higher temperatures. The greater Q_{10L} at the TSL than SSL under all grasses was associated with higher C_L concentrations as well as specific activities of DHA and GLU at the TSL. The similar Q_{10L} of bulk soils at the TSL and SSL could be ascribed to the similar proportion of C_L (~63-65%) at both soil layers, leading to consistent substrate availability at both soil layers. However, lower Q_{10L} of bulk soils compared with aggregates could be related to lower concentration of C_L in bulk soils than aggregates (Fig. 2B)

The greater Q_{10R} values in MA, MI, and SC of V.ziz, C.ful, and P.max than other grasses could also be linked to poor soil aggregation, greater specific activities of PHOX and PEROX, and higher degree of decomposition of SOM. The higher Q_{10R} values in MI over MA and SC could

be ascribed to MI formation mechanisms and greater concentration of C_R within MI. Recalcitrant substrates requiring high activation energy will decompose more readily at higher temperatures than labile substrates requiring low activation energy (Conant et al., 2011) because fine particles associated with MI have the ability to strongly adsorb labile organic substances through a variety of mechanisms (e.g. ligand exchange, polyvalent cation bridges, and large surface areas) (Wankhede et al., 2020). Resultantly, MI had a higher Q_{10R} than SC and MA. Higher C_R concentrations were linked to Q_{10R} of MA, MI, and SC being higher at the TSL than SSL (Liu et al., 2015). Thus, our first hypothesis was accepted as labile carbon concentration had direct control on the Q_{10L}, whereas, Q_{10R} was governed by the quantity of recalcitrant carbon.

Generally speaking, organic matter becomes more chemically resistant as soil depth increases. Thus, according to theory, Q_{10} should rise with depth (Karhu et al., 2010). Our findings, however, contradicted this hypothesis, indicating that processes other than chemical recalcitrance are required to account for our findings. According to published literatures, there are two potential reasons of declining Q_{10} at the SSL: (1) the greater protection of SOC at the SSL restricts its availability to microbes, and (2) the nature of the microbial community changes with depth. Firstly, the proportion of physically protected SOC rises at the SSL due to association with soil minerals, specifically with SC (Schrumpf et al. 2013), creating a physical disconnection between microbes and substrates, leading to a lesser dependence of microbial respiration on temperature in subsoils (Conant et al. 2011). The C_R contents within soil aggregates may reveal the degree of physically protected SOC against microbial breakdown. The proportion of C_R within MA was 10% higher at the SSL than TSL (Table 1). Consequently, one of the reasons causing the declining Q_{10} with depth may be the increased substrate constraint for microbes brought on by the physical protection of SOC. Secondly, the temperature sensitivity of microbial respiration at different depths may be partially explained by the different microbial activities at different depths, as indicated by the changes in specific

activities of enzymes (Fig. 4A and 4B) (Stone et al. 2014). According to the correlation study, C_L and C_R had a significant role in influencing Q_{10L} and Q_{10R} at various depths, respectively (Table 5). The variation in Q_{10} values may be directly caused by changes in community composition, which are probably linked to variations in C_L and C_R at two depths; as indicated by the differential specific activity of DHA, GLU, PHOX, and PEROX.

We found that Q_{10L} values were higher than Q_{10R} within aggregates due to strong influence of Q_{10R} on Q_{10L} as indicated by SEM (Fig. 6). This could possibly be due to increase of C_L at higher temperature due to a boost in the enzymatic activity accelerating decay of recalcitrant pools of SOM. Two major groups of enzymes, namely, oxidative and hydrolytic enzymes play pivotal roles in decomposing SOM. Oxidative enzymes transform aromatic and phenolic polymers to relatively labile substances, which are further decomposed by hydrolytic enzymes. Greater activities of oxidative enzymes (PHOX and PEROX) at high temperature assisted in providing greater microbial access to the recalcitrant SOM, and, therefore, resulting in an increased C_L (Waldrop and Firestone, 2004). This mechanism might have ensured the labile substrate supply by offsetting it depletion in substrate-limited degraded land at higher temperatures and resulted in greater increase of k_L over k_R. Consequently, Q_{10L} values were higher than Q_{10R} within aggregates.

The higher Q_{10L} over Q_{10R} was also reported by previous researchers (Zhu and Cheng 2011). It was demonstrated by Larionova et al. (2007) that the concentration of rapidly decomposable carbon affects how temperature affects microbial respiration. In addition, Fissore et al. (2013) found that labile substrate-depleted soils with prolonged incubation had a reduced temperature dependency of SOC decomposition compared to non-depleted soils or substrate-depleted soils treated with saturated glucose. The function of C_L in regulating the temperature sensitivity of microbiological respiration in soils is strongly supported by all of these investigations. Additionally, environmental restrictions on decomposition can decrease substrate availability

and lessen the intrinsic temperature sensitivity of SOC decomposition, according to recent syntheses (Davidson and Janssens 2006; Conant et al., 2011). By demonstrating higher Q_{10L} than Q_{10R} within aggregates at the TSL and SSL in ecologically restored grass covers, our current work advanced the understanding of Q_{10} in restored land. This study demonstrated how C_L concentration in bulk soils and aggregates affects SOC mineralization in response to warming. All of these factors would contribute to the growing understanding of the mechanismsthat could play a major role in determining its persistence in a warming environment (Conant et al., 2011).

Root C quality and soil C quality or quantity: The governing factor behind temperature sensitivity of soil C in semi-arid restored land

Our results indicated that root and soil C quality exerted contrasting controls on the Q_{10} of SOC fractions. At the topsoil, root litter carboxylates and polysaccharides enhanced Q_{10} of labile C, consistent with the view that readily available substrates stimulated microbial activities and amplified temperature responses (Figs. 3 and 4) (Blagodatskaya et al., 2016; Qin et al., 2019). In contrast, SOM aromaticity was negatively associated with labile-C Q_{10}, reflecting the chemical recalcitrance and mineral protection of aromatic compounds that limit microbial access (Leifeld et al., 2014). By comparison, Q_{10} of recalcitrant SOC was positively related to the humification index, decomposition degree of SOM, and aromatic/phenolic compounds of roots (Fig. 5), in line with the higher activation energy required to decompose chemically complex substrates (Qin et al., 2019). At the subsoil, however, root litter chemistry had little effect, likely due to lower root inputs and microbial activity, while SOM quality and pool size had the dominant control on Q_{10} (Blagodatskaya et al., 2016). Together, these findings suggested that labile inputs might increase the short-term temperature sensitivity of SOC, whereas chemically complex substrates could lead to higher Q_{10} in recalcitrant pools, with depth-dependent shifts in the relative importance of root- versus soil-derived controls.

583 At the TSL, quantity of root litter is greater than that at the SSL, leading to higher supply of
584 labile compounds. In other words, labile compound supply at the TSL is less limiting than that
585 at the SSL. Hence, at the TSL, quality of root litter played an influential role on Q_{10L} and Q_{10R}.
586 However, a theoretical relationship between labile substrate availability and the temperature
587 sensitivity of SOC decomposition could be derived using the Michaelis–Menten model. In this
588 model, both Vmax (maximal rate of enzymatic activity) and Km (dissociation constant or half-
589 saturation constant) are positively temperature dependent. Therefore, the relative importance
590 of Km for estimation of soil C mineralization rate is reduced when labile substrate is added in
591 initially labile substrate limited soil. The lower concentration of C_L at the SSL and the reduced
592 relative importance of Km with slight increase in C_L the Q_{10L} becomes solely dependent upon
593 the C_L at the SSL (Fissore et al., 2013; Pang et al., 2014). The higher amount of root litter at
594 the TSL assured greater supply of carboxylates, polysaccharides, aromatic and phenolic
595 compounds, resulting in a greater influence of Km on Q_{10L} and Q_{10R} at the TSL than that at the
596 SSL. This led to a combined influence of labile substrate quality and quantity on Q_{10L} at the
597 TSL only. Thus, our second hypothesis—that availability of labile substrate has a greater
598 impact on Q_{10L} after root litter decomposition than substrate quality, with substrate quality
599 alone not being able to explain variation in Q_{10L}—was supported by the positive correlation of
600 Q_{10L} with carboxylates and polysaccharides of root litter and its negative correlation with
601 aromaticity of SOM (Fig. 7).

602 The structural equation model clearly revealed that influence of C_L and C_R was significantly
603 higher on Q_{10L} and Q_{10R}, respectively, at the TSL and SSL. It also indicated that at the TSL,
604 Q_{10L} was influenced by C_L and root C quality parameters; whereas, at the SSL, it was only
605 impacted by C_L, although Q_{10R} continued to be influenced by C_R and SOC quality parameters
606 (Fig. 6). The question if Q_{10L} and Q_{10R} change with substrate quality is one that is hotly
607 contested in SOC decomposition. According to the CQT theory, Q_{10} should rise as recalcitrance
608 increases (Davidson and Janssens, 2006). Our results generally contradicted the theory. This

609 disparity might result from failing to consider how labile substrate supply influences C
610 mineralization reactions in previous studies (Gershenson et al., 2009). The kinetic theory of
611 decomposition and the CQT hypothesis were both supported by the significant correlations
612 found in our study between Q_{10R} and the HI and aromaticity of SOM and the aromatic and
613 phenolic substances of root litter (Table 5). Thus, the observed difference in Q_{10R} can be
614 explained exclusively by substrate quality (Craine et al., 2010; Eberwein et al., 2015). The
615 dependence of Q_{10R} on substrate quality in addition to C_R could be linked to substrate chemistry.
616 The recalcitrant pools of SOM comprised of lignin-derived compounds as exhibited by the
617 stronger peaks at 1512 cm^{-1} (Kostryukov et al., 2023). Furthermore, the FTIR analysis in this
618 work (Fig. S2 and S3) also indicated, similar to previous researches, that the primary chemical
619 elements contributing to aromatic carbons in litter and SOM can actually be quite different
620 depending on the type of vegetation (Nierop et al., 2006; Obeng et al., 2023). Both relatively
621 high-quality molecules, such as hydrolysable tannins (1610, 1510, and 1450 cm^{-1}) or aromatic
622 amino acids (1340–1250 cm^{-1}), and lower-quality structural components, like lignin, condensed
623 tannins, and suberin (921, 2852, 1737, 1242, 1158 and 724 cm^{-1}), might compose the aromatic
624 compounds (Fig. S2 and S3). The distinct link between aromatic compounds and Q_{10L} and Q_{10R}
625 may thus be due in part to differences in the amount and composition of aromatic amino acids
626 between litter and SOM. According to the FTIR absorbance spectroscopy, the average
627 concentration of carboxylate and polysaccharide in root litter was higher than that in SOM; the
628 content of these compounds was clearly declining as the litter degraded. In spite of this, the C
629 fraction was dominated by carboxylate and polysaccharide, suggesting that a sizable part of the
630 carbons in carboxylate and polysaccharide make up a rather labile carbon pool. This would
631 also account for a rising Q_{10L} when the contents of polysaccharides and carboxylates increase.
632 The lower Q_{10R} than Q_{10L} in aggregates could also be caused by the rapid depletion of readily
633 available labile compounds within aromatic substrate at higher temperature. The increased
634 amount of lignin, tannins, suberin, etc. could indicate a shift towards decomposition of more

complex plant structural compounds (ligno-cellulose), resulting in the dependence of Q_{10R} on substrate quality parameters.Thus, our third hypothesis—that changes in Q_{10L} and Q_{10R} would be differently influenced by root litter C and soil C quality due to their variable chemical recalcitrance, physical protection, and enzymatic decomposition mechanisms —is supported by the variable correlations of C_L and C_R with Q_{10L} and Q_{10R}, respectively (Fig. 7) (Davidson and Janssens, 2006).

Limitations and implications of the study

The generalisation of our findings should be done with care because (i) the duration of incubation was most likely insufficient for thermal adaptation of microbial community; (ii) the study lacks the influence of soil moisture fluctuation; and (iii) our research had a small sample size as well as soil type. Therefore, it is necessary to validate the association between SOM and root C chemistry, as well as Q_{10L} and Q_{10R}, utilising diverse soils and methodologies. Most significantly, the conclusion drawn from the present approach is restricted to the ecologically restored degraded land.

The results from this study indicated that changes in SOC stability in ecologically restored land under grasses with regular litter input and higher temperatures will be highly dependent on labile C content in bulk soils and aggregates. Thus, soil C cycling models that explicitly incorporate factors that influences the protection and accessibility of C as well as microbial acclimation in the soil matrix should improve prediction of SOC dynamics in response to enhanced aboveground litter input and elevated temperature.

Conclusions

In consequence to the first objective this study demonstrated the effect grass covers on Q_{10} of SOC decomposition in restored land under warming environment due to of variations substrate availability. The Q_{10L} and Q_{10R} was also impacted by soil aggregation and enzyme activity. This

led to a lower Q_{10L} and Q_{10R} under C.cil, H.con, and S.ner over other grasses, indicating that these grass covers could contribute to greater SOC storage under warming situations. In realtion to the second objective, we found that Q_{10L} and Q_{10R} of macroaggregate was lower than microaggregate, indicating that long-term restoration activity that promote macroaggregate formation would facilitate greater macroaggregate formation and consequently C sequestration under a rising temperature scenario. The Q_{10L} and Q_{10R} was significantly influenced by labile and recalcitrant C contents under all grass covers at both soil layers. Furthermore, Q_{10L} and Q_{10R} was impacted by root litter C quality at the topsoil only, indicating that the Q_{10} of SOC decomposition in sub-surface soil layer with low substrate availability might be enhanced more by labile C input. Furthermore, the positive relationship between Q_{10L} and Q_{10R} with labile and recalcitrant C contradicted the CQT hypothesis in restored degraded soils, which had low initial C content. Therefore, C-climate models based on the CQT hypothesis should be used cautiously when predicting soil C dynamics in future studies. The observed variations in Q_{10L} and Q_{10R} highlight the important role of substrate availability in soil C cycles, and future earth system model should take this into consideration because labile C is continuously added into soil via root exudates or plant litter in the field.

Funding

"The authors declare that no funds, grants, or other financial supports were received during the preparation of this manuscript."

Conflict of Interest

"The authors have no relevant financial or non-financial interests to disclose."

Author Contributions

"All authors contributed to the study conception and design. Material preparation, data collection and analysis were performed by Vikas K Singhal, Deepak Ojha and Sourav Kumar.

683 The first draft of the manuscript was written by Avijit Ghosh and all authors commented on
684 previous versions of the manuscript. All authors read and approved the final manuscript."

685 **Data Availability**

686 "The datasets generated during and/or analysed during the current study are available from the
687 corresponding author on reasonable request."

688 **Acknowledgment**

689 The authors are pleased to acknowledge the help, support, and motivation received from
690 Director, ICAR-IGFRI, Jhansi and Vice Chancellor and Director Education, RLBCAU, Jhansi
691 to conduct the research work. The publication is referenced under ICAR-IGFRI/PME
692 Reference letter/Research Paper/03/2025. The authors express their sincere gratitude to the
693 anonymous reviewers for reviewing the manuscript.

694 **References**

695 Anderson, J.P., 1982. Soil respiration. *Methods of soil analysis: part 2 chemical and*
696 *microbiological properties*, *9*, pp.831-871.

697 Blagodatskaya, E., Blagodatsky, S., Anderson, T. H., & Kuzyakov, Y. (2016). Microbial growth
698 and carbon use efficiency in the rhizosphere and root-free soil. *PLoS ONE, 11*(8),
699 e0163457. https://doi.org/10.1371/journal.pone.0163457

700 Qin, S., Chen, L., Fang, K., Zhang, Q., Wang, J., Guo, X., ... & Yang, Y. (2019). Temperature
701 sensitivity of SOM decomposition governed by aggregate protection and microbial
702 communities. *Global Change Biology, 25*(12), 3926–3940.
703 https://doi.org/10.1111/gcb.14850

704 Leifeld, J., Von Lützow, M., Kögel-Knabner, I., & Ekschmitt, K. (2014). A conceptual approach
705 to the quality–temperature relationship of organic matter decomposition. *Soil Biology and*
706 *Biochemistry, 74,* 60–68. https://doi.org/10.1016/j.soilbio.2014.02.021

707 Bracho, R., Natali, S., Pegoraro, E., Crummer, K.G., Schädel, C., Celis, G., Hale, L., Wu, L.,
708 Yin, H., Tiedje, J.M. and Konstantinidis, K.T., 2016. Temperature sensitivity of organic
709 matter decomposition of permafrost-region soils during laboratory incubations. *Soil*
710 *Biology and Biochemistry*, *97*, pp.1-14.

711 Bucka, F.B., Kölbl, A., Uteau, D., Peth, S. and Kögel-Knabner, I., 2019. Organic matter input
712 determines structure development and aggregate formation in artificial
713 soils. *Geoderma*, *354*, p.113881.

Canisares, L.P., Banet, T., Rinehart, B., McNear, D. and Poffenbarger, H., 2023. Litter quality and living roots affected the formation of new mineral-associated organic carbon but did not affect total mineral-associated organic carbon in a short-term incubation. *Geoderma*, *430*, p.116302.

Conant, R.T., Ryan, M.G., Ågren, G.I., Birge, H.E., Davidson, E.A., Eliasson, P.E., Evans, S.E., Frey, S.D., Giardina, C.P., Hopkins, F.M. and Hyvönen, R., 2011. Temperature and soil organic matter decomposition rates–synthesis of current knowledge and a way forward. *Global change biology*, *17*(11), pp.3392-3404.

Craine, J.M. and Gelderman, T.M., 2011. Soil moisture controls on temperature sensitivity of soil organic carbon decomposition for a mesic grassland. *Soil Biology and Biochemistry*, *43*(2), pp.455-457.

Crowther, T.W., Todd-Brown, K.E., Rowe, C.W., Wieder, W.R., Carey, J.C., Machmuller, M.B., Snoek, B.L., Fang, S., Zhou, G., Allison, S.D. and Blair, J.M., 2016. Quantifying global soil carbon losses in response to warming. *Nature*, *540*(7631), pp.104-108.

Davidson, E.A. and Janssens, I.A., 2006. Temperature sensitivity of soil carbon decomposition and feedbacks to climate change. *Nature*, *440*(7081), pp.165-173.

Deng, L., Kim, D.G., Peng, C. and Shangguan, Z., 2018. Controls of soil and aggregate-associated organic carbon variations following natural vegetation restoration on the L oess P lateau in China. *Land Degradation & Development*, *29*(11), pp.3974-3984.

Dick, R.P., 2011, September. Methods of soil enzymology. Madison: Soil Science Society of America.

Fang, X.M., Chen, F.S., Wan, S.Z., Yang, Q.P. and Shi, J.M., 2015. Topsoil and deep soil organic carbon concentration and stability vary with aggregate size and vegetation type in subtropical China. *PLoS One*, *10*(9), p.e0139380.

Fierer, N., Colman, B. P., Schimel, J. P., & Jackson, R. B., 2006. Predicting the temperature dependence of microbial respiration in soil: A continental-scale analysis. *Global Biogeochemical Cycles*, *20*(3).

Fissore, C., Giardina, C.P. and Kolka, R.K., 2013. Reduced substrate supply limits the temperature response of soil organic carbon decomposition. *Soil Biology and Biochemistry*, *67*, pp.306-311.

Fissore, C., Giardina, C.P. and Kolka, R.K., 2013. Reduced substrate supply limits the temperature response of soil organic carbon decomposition. *Soil Biology and Biochemistry*, *67*, pp.306-311.

Friedlingstein, P., Cox, P., Betts, R., Bopp, L., von Bloh, W., Brovkin, V., Cadule, P., Doney, S., Eby, M., Fung, I. and Bala, G., 2006. Climate–carbon cycle feedback analysis: results from the C4MIP model intercomparison. *Journal of climate*, *19*(14), pp.3337-3353.

Frøseth, R.B. and Bleken, M.A., 2015. Effect of low temperature and soil type on the decomposition rate of soil organic carbon and clover leaves, and related priming effect. *Soil Biology and Biochemistry*, *80*, pp.156-166.

Ghosh, A., Das, A., Das, D., Ray, P., Bhattacharyya, R., Biswas, D.R. and Biswas, S.S., 2020. Contrasting land use systems and soil organic matter quality and temperature sensitivity in North Eastern India. *Soil and Tillage Research*, *199*, p.104573.

Ghosh, A., Kumar, S., Kushwaha, B.P., Lal, R., Singh, A.K., Yadav, V.K. and Chandra, A., 2025. Impact of short-term pasture development on soil aggregation, temperature sensitivity of soil organic carbon, and functional diversity in semi-arid ecosystem. *Arid Land Research and Management*, pp.1-27.

Hontoria, C., Gómez-Paccard, C., Mariscal-Sancho, I., Benito, M., Pérez, J. and Espejo, R., 2016. Aggregate size distribution and associated organic C and N under different tillage systems and Ca-amendment in a degraded Ultisol. *Soil and Tillage Research*, *160*, pp.42-52.

Jackson, O., Quilliam, R.S., Stott, A., Grant, H. and Subke, J.A., 2019. Rhizosphere carbon supply accelerates soil organic matter decomposition in the presence of fresh organic substrates. *Plant and Soil*, *440*, pp.473-490.

Karhu, K., Fritze, H., Tuomi, M., Vanhala, P., Spetz, P., Kitunen, V. and Liski, J., 2010. Temperature sensitivity of organic matter decomposition in two boreal forest soil profiles. *Soil Biology and Biochemistry*, *42*(1), pp.72-82.

Kleber, M., Nico, P.S., Plante, A., Filley, T., Kramer, M., Swanston, C. and Sollins, P., 2011. Old and stable soil organic matter is not necessarily chemically recalcitrant: implications for modeling concepts and temperature sensitivity. *Global change biology*, *17*(2), pp.1097-1107.

Kostryukov, S.G., Matyakubov, H.B., Masterova, Y.Y., Kozlov, A.S., Pryanichnikova, M.K., Pynenkov, A.A. and Khluchina, N.A., 2023. Determination of lignin, cellulose, and hemicellulose in plant materials by FTIR spectroscopy. *Journal of Analytical Chemistry*, *78*(6), pp.718-727.

Larionova, A.A., Yevdokimov, I.V. and Bykhovets, S.S., 2007. Temperature response of soil respiration is dependent on concentration of readily decomposable C. *Biogeosciences*, *4*(6), pp.1073-1081.

Lavallee, J.M., Soong, J.L. and Cotrufo, M.F., 2020. Conceptualizing soil organic matter into particulate and mineral-associated forms to address global change in the 21st century. *Global change biology*, *26*(1), pp.261-273.

Liu, N., Kan, H.M., Yang, G.W. and Zhang, Y.J., 2015. Changes in plant, soil, and microbes in a typical steppe from simulated grazing: explaining potential change in soil C. *Ecological Monographs*, *85*(2), pp.269-286.

Liu, Y., Xu, L., Zheng, S., Chen, Z., Cao, Y., Wen, X. and He, N., 2021. Temperature sensitivity of soil microbial respiration in soils with lower substrate availability is enhanced more by labile carbon input. *Soil Biology and Biochemistry*, *154*, p.108148.

Ma, Y., McCormick, M.K., Szlavecz, K. and Filley, T.R., 2019. Controls on soil organic carbon stability and temperature sensitivity with increased aboveground litter input in deciduous forests of different forest ages. *Soil Biology and Biochemistry*, *134*, pp.90-99.

Magh, T., Mozhui, L., Kakati, L.N., Ao, B., Lemtur, T. and Jing, L., 2024. Litter decomposition and nutrient dynamics in a subtropical ecosystem: A comparison of natural and plantation forests (Duabanga grandiflora) in Nagaland, North-East India. *Global Ecology and Conservation*, *56*, p.e03321.

Nierop, K.G., Verstraten, J.M., Tietema, A., Westerveld, J.W. and Wartenbergh, P.E., 2006. Short-and long-term tannin induced carbon, nitrogen and phosphorus dynamics in Corsican pine litter. *Biogeochemistry*, *79*, pp.275-296.

Obeng, A.S., Dunne, J., Giltrap, M. and Tian, F., 2023. Soil organic matter carbon chemistry signatures, hydrophobicity and humification index following land use change in temperate peat soils. *Heliyon*, *9*(9).

Pang, X., Zhu, B., Lü, X. and Cheng, W., 2015. Labile substrate availability controls temperature sensitivity of organic carbon decomposition at different soil depths. *Biogeochemistry*, *126*, pp.85-98.

Patidar, P., Sannagoudar, M.S., Ghosh, A., Singh, A.K., Misra, S., Khandibagur, V., Ojha, D., Casini, R., Elansary, H.O. and Chandra, A., 2023. Tropical range grasses can sustain soil functions despite nutrient depletion in semiarid degraded land. *Frontiers in Sustainable Food Systems*, *7*, p.1230156.

Peng, X., Huang, Y., Duan, X., Yang, H. and Liu, J., 2023. Particulate and mineral-associated organic carbon fractions reveal the roles of soil aggregates under different land-use types in a karst faulted basin of China. *Catena*, *220*, p.106721.

Perkins, L.B. and Nowak, R.S., 2013. Native and non-native grasses generate common types of plant–soil feedbacks by altering soil nutrients and microbial communities. *Oikos*, *122*(2), pp.199-208.

Phillips, R.P., Finzi, A.C. and Bernhardt, E.S., 2011. Enhanced root exudation induces microbial feedbacks to N cycling in a pine forest under long-term CO2 fumigation. *Ecology letters*, *14*(2), pp.187-194.

Qiu, L., Wei, X., Gao, J. and Zhang, X., 2015. Dynamics of soil aggregate-associated organic carbon along an afforestation chronosequence. *Plant and Soil*, *391*, pp.237-251.

Rovira, P. and Vallejo, V.R., 2002. Labile and recalcitrant pools of carbon and nitrogen in organic matter decomposing at different depths in soil: an acid hydrolysis approach. *Geoderma*, *107*(1-2), pp.109-141.

Sarkar, B., Singh, M., Mandal, S., Churchman, G.J. and Bolan, N.S., 2018. Clay minerals—Organic matter interactions in relation to carbon stabilization in soils. In *The future of soil carbon* (pp. 71-86). Academic Press.

Schrumpf, M., Kaiser, K., Guggenberger, G., Persson, T., Kögel-Knabner, I. and Schulze, E.D., 2013. Storage and stability of organic carbon in soils as related to depth, occlusion within aggregates, and attachment to minerals. *Biogeosciences*, *10*(3), pp.1675-1691.

Singhal, V.K., Ghosh, A., Singh, A.K., Singh, Y., Biswas, S.S., Ojha, D. and Bhattacharyya, R., 2025. How grasses stabilize soil organic carbon in aggregates of semi-arid ecologically restored land: Evidence from 13C natural abundance. *Catena*, *249*, p.108627.

Six, J., Paustian, K., Elliott, E.T. and Combrink, C., 2000. Soil structure and organic matter I. Distribution of aggregate-size classes and aggregate-associated carbon. *Soil Science Society of America Journal*, *64*(2), pp.681-689.

Stone, M.M., DeForest, J.L. and Plante, A.F., 2014. Changes in extracellular enzyme activity and microbial community structure with soil depth at the Luquillo Critical Zone Observatory. *Soil Biology and Biochemistry*, *75*, pp.237-247.

Wagai, R., Kishimoto-Mo, A.W., Yonemura, S., Shirato, Y., Hiradate, S. and Yagasaki, Y., 2013. Linking temperature sensitivity of soil organic matter decomposition to its molecular structure, accessibility, and microbial physiology. *Global Change Biology*, *19*(4), pp.1114-1125.

Wankhede, M., Ghosh, A., Manna, M.C., Misra, S., Sirothia, P., Rahman, M.M., Bhattacharyya, P., Singh, M., Bhattacharyya, R. and Patra, A.K., 2020. Does soil organic carbon quality or quantity govern relative temperature sensitivity in soil aggregates?. *Biogeochemistry*, *148*, pp.191-206.

Xiao, L., Yao, K., Li, P., Liu, Y., Chang, E., Zhang, Y. and Zhu, T., 2020. Increased soil aggregate stability is strongly correlated with root and soil properties along a gradient of secondary succession on the Loess Plateau. *Ecological Engineering*, *143*, p.105671.

Xu, W., Li, W., Jiang, P., Wang, H. and Bai, E., 2014. Distinct temperature sensitivity of soil carbon decomposition in forest organic layer and mineral soil. *Scientific Reports*, *4*(1), p.6512.

Yang, H., Long, H., Li, X., Luo, X., Liao, Y., Wang, C., Cai, H. and Shu, Y., 2024. Vegetation restoration improved aggregation stability and aggregated-associated carbon preservation in the karst areas of Guizhou Province, southwest China. *PeerJ*, *12*, p.e16699.

Zacháry, D., Filep, T., Jakab, G., Varga, G., Ringer, M. and Szalai, Z., 2018. Kinetic parameters of soil organic matter decomposition in soils under forest in Hungary. *Geoderma regional*, *14*, p.e00187.

Zhong, Z., Wu, S., Lu, X., Ren, Z., Wu, Q., Xu, M., Ren, C., Yang, G. and Han, X., 2021. Organic carbon, nitrogen accumulation, and soil aggregate dynamics as affected by vegetation restoration patterns in the Loess Plateau of China. *Catena*, *196*, p.104867.

Zhu, B. and Cheng, W., 2011. Rhizosphere priming effect increases the temperature sensitivity of soil organic matter decomposition. *Global Change Biology*, *17*(6), pp.2172-2183.

Zhu, G.Y., Shangguan, Z.P. and Deng, L., 2017. Soil aggregate stability and aggregate-associated carbon and nitrogen in natural restoration grassland and Chinese red pine plantation on the Loess Plateau. *Catena*, *149*, pp.253-260.

Table 1. Impact of grass covers on bulk soil and aggregate associated labile and recalcitrant carbon (C_L and C_R) at top (TSL) and sub-surface (SSL) soil layers in semi-arid restored land

	BS		MA		MI		SC	
				C_L (mg $100g^{-1}$)				
	TSL	SSL	TSL	SSL	TSL	SSL	TSL	SSL
C.cil[#]	114.1a[$]	92.5a	244.1a	129.6ab	297.0a	217.4a	233.2a	142.0a
P.max	88.8c	83.9a	226.6b	120.6b	271.6b	176.9c	203.3b	94.4c
C.ful	88.2c	43.8c	217.0b	71.4d	246.7c	179.6c	165.8c	92.7c
H.con	90.1c	61.7b	248.2a	109.6c	243.4c	200.3b	201.2b	123.8b
S.ner	106.1b	87.0a	255.8a	137.5a	272.3b	220.8a	232.2a	148.9a
V.ziz	83.9c	52.4b	146.1c	56.3e	254.5c	119.6d	146.4d	72.9d
URC	63.5d	36.4c	91.3d	82.8d	86.4d	67.6e	40.4e	52.3e
				C_R (mg $100g^{-1}$)				
	TSL	SSL	TSL	SSL	TSL	SSL	TSL	SSL
C.cil	67.9a	54.5a	216.3a	114.8a	267.6b	138.6a	292.9a	172.3a
P.max	52.2b	49.1b	154.8c	70.4d	220.5c	111.0bc	245.7c	155.0b
C.ful	51.8b	24.2d	136.3d	57.9e	181.9d	108.4c	232.4c	133.6c
H.con	52.9b	35.3c	187.6b	119.5b	257.7b	119.5b	274.6b	161.9a
S.ner	62.9a	51.0ab	180.1b	106.1c	292.3a	135.2a	281.7ab	165.0a
V.ziz	49.1b	29.6cd	88.4e	70.3d	133.3e	127.5ab	180.6d	127.5c
URC	36.5c	19.6e	45.4f	36.5f	53.3f	61.7d	33.1e	70.1d

[#]*See materials and methods for details*

[$]*Statistical inference according to Tukey's test is shown by lowercase letters.*

Table 2 Impact of grass covers on decay rates of labile ($k_L \times 10^{-2}$ mg C day^{-1}) and recalcitrant ($k_R \times 10^{-2}$ mg C day^{-1}) pools of soil organic carbon from bulk soils, macroaggregate (MA), microaggregate (MI), and silt plus clay (SC) at top (TSL) and sub-surface (SSL) soil layers in semi-arid restored land.

TSL																								
Soil fraction	Bulk soil			MA			MI			SC			Bulk soil			MA			MI			SC		
Decay rate	k_L			k_L			k_L			k_L			k_R			k_R			k_R			k_R		
Temperature (°C)	25	32	37	25	32	37	25	32	37	25	32	37	25	32	37	25	32	37	25	32	37	25	32	37
C.cil[#]	1.42e[$]	1.77f	1.86g	0.24c	0.24c	0.45c	0.19d	0.39d	0.97e	0.24e	0.42f	0.81e	0.25b	0.31b	0.42b	0.23b	0.29b	0.40b	0.27b	0.36b	0.51b	0.25b	0.37c	0.47c
P.max	2.95c	4.16c	4.52d	0.40b	0.56b	1.51b	0.30c	0.79c	2.49c	0.41d	0.91d	2.19c	0.31a	0.34ab	0.43b	0.29a	0.36a	0.50a	0.34a	0.44a	0.63a	0.31a	0.46b	0.58b
C.ful	2.95c	4.32c	5.08c	0.44b	0.63b	1.73b	0.38b	1.01b	3.28b	0.56c	1.12c	2.45c	0.31a	0.36a	0.46ab	0.28a	0.36a	0.49a	0.34a	0.44a	0.62a	0.31a	0.45b	0.58b
H.con	2.36b	3.08d	3.38e	0.26c	0.28c	0.60cd	0.27cd	0.52c	1.23de	0.32e	0.55e	1.03d	0.26b	0.32ab	0.43ab	0.23b	0.30b	0.41b	0.28b	0.37b	0.53b	0.26b	0.38c	0.49c
S.ner	1.78d	2.36e	2.60f	0.26c	0.31c	0.72d	0.23d	0.45cd	1.09d	0.27e	0.51e	1.08d	0.27b	0.33ab	0.44ab	0.25ab	0.31b	0.43b	0.29b	0.39b	0.55ab	0.27b	0.40c	0.51c
V.ziz	3.24a	4.80b	5.78b	0.68a	0.97a	1.70b	0.40b	1.22a	4.49a	0.76b	1.63b	3.84b	0.30a	0.36a	0.48a	0.28a	0.35a	0.49a	0.33a	0.44a	0.61a	0.34a	0.51a	0.64a
URC	5.35a	5.72a	7.01a	0.69a	1.06a	3.18a	0.53a	0.93b	3.25b	2.36a	3.82a	4.77a	0.29a	0.35a	0.48a	0.28a	0.36a	0.49a	0.33a	0.44a	0.62a	0.31a	0.45b	0.58b
SSL																								
Soil fraction	Bulk soil			MA			MI			SC			Bulk soil			MA			MI			SC		
Decay rate	k_L			k_L			k_L			k_L			k_R			k_R			k_R			k_R		
Temperature (°C)	25	32	37	25	32	37	25	32	37	25	32	37	25	32	37	25	32	37	25	32	37	25	32	37
C.cil	2.12d	2.89d	2.98f	0.64e	1.28d	1.65e	0.31d	0.49c	0.91e	0.49e	0.59e	0.83f	0.24a	0.33b	0.35b	0.17b	0.20b	0.27b	0.20b	0.25b	0.33b	0.19b	0.25b	0.34b
P.max	3.80c	5.63c	6.31d	1.10c	1.88b	3.55b	0.58bc	1.12a	2.49a	1.16c	1.42c	2.03d	0.26a	0.36a	0.38a	0.21a	0.25a	0.33a	0.25a	0.30a	0.40a	0.23a	0.31a	0.41a
C.ful	4.60b	6.95a	8.13a	1.70b	1.62c	2.64c	0.56c	1.09a	2.44a	1.28c	1.68c	2.57c	0.27a	0.36a	0.39a	0.21a	0.25a	0.32a	0.24a	0.29a	0.39a	0.23a	0.30a	0.41a
H.con	4.82b	6.63a	6.95c	0.83d	1.18d	1.42f	0.38d	0.67b	1.41c	0.64d	0.77d	1.12e	0.24a	0.33b	0.36b	0.18b	0.21b	0.27b	0.21b	0.26b	0.37ab	0.19b	0.26a	0.37ab
S.ner	2.44d	3.40e	3.58e	0.65e	1.46cd	2.15d	0.32d	0.57bc	1.18d	0.51d	0.69de	1.10e	0.25a	0.34b	0.36b	0.18b	0.22b	0.28b	0.21b	0.27ab	0.36ab	0.20b	0.27ab	0.37ab
V.ziz	5.39a	6.17b	7.18c	1.08c	1.30d	1.69e	0.73a	1.10a	1.90b	1.83b	2.11b	2.86b	0.27a	0.36a	0.39a	0.21a	0.25a	0.32a	0.24a	0.29a	0.39a	0.23a	0.30a	0.41a
URC	5.54a	6.61a	7.72b	2.51a	2.79a	4.00a	0.63b	0.64b	1.25d	3.19a	3.54a	3.77a	0.27a	0.37a	0.39a	0.21a	0.25a	0.32a	0.24a	0.30a	0.41a	0.23a	0.30a	0.42a

[#]*See materials and methods for details*

[$]*Statistical inference according to Tukey's test is shown by lowercase letters.*

879 Table 3 Impact of grass covers on temperature sensitivity of labile (Q_{10L}) and recalcitrant (Q_{10R})
880 pools of soil organic carbon in bulk soils (BS), macroaggregate (MA), microaggregate (MI),
881 and silt plus clay (SC) at top (TSL) and sub-surface (SSL) soil layers in semi-arid restored land.

	Q_{10L}							
	BS		MA		MI		SC	
	TSL	SSL	TSL	SSL	TSL	SSL	TSL	SSL
C.cil[#]	1.26c[$]	1.34bc	1.65d	2.24c	2.73cd	2.07c	2.69ab	1.53c
P.max	1.44b	1.54a	2.92b	2.62a	3.06b	2.98s	2.81a	1.58c
C.ful	1.58a	1.62a	3.00b	2.40b	2.91c	2.60b	2.54b	1.76b
H.con	1.36bc	1.37b	1.9d	1.57d	2.41e	2.56b	2.61b	1.57c
S.ner	1.38bc	1.39b	2.23c	1.73d	2.60c	2.53b	2.64b	1.89a
V.ziz	1.63a	1.27c	3.04b	2.45b	3.28a	1.84d	2.78a	1.44cd
URC	1.24	1.32bc	3.43a	2.45b	3.33a	1.36e	1.81c	1.38d
	Q_{10R}							
	BS		MA		MI		SC	
	TSL	SSL	TSL	SSL	TSL	SSL	TSL	SSL
C.cil	1.53a	1.38d	1.59c	1.65c	1.68c	1.50cd	1.71c	1.45b
P.max	1.30c	1.68b	1.89b	1.42d	2.65b	1.65b	1.98a	1.62a
C.ful	1.40b	1.69b	1.97b	1.62c	2.65b	1.68b	1.83b	1.63a
H.con	1.54a	1.44cd	1.58c	1.44d	1.67c	1.46d	1.70c	1.41b
S.ner	1.49ab	1.48c	1.57c	1.43d	1.66c	1.54c	1.69c	1.47b
V.ziz	1.44b	1.39d	2.01b	1.74b	2.65b	1.79a	1.84b	1.63a
URC	1.53a	1.79a	2.40a	1.84a	2.96a	1.68b	2.07a	1.66a

882 [#]*See materials and methods for details*
883 [$]*Statistical inference according to Tukey's test is shown by lowercase letters.*
884
885

Table 4 Impact of grass covers on quality parameters (humification index: HI; aromaticity; and degree of decomposition: DDI) of soil organic matter in bulk soils (BS), macroaggregate (MA), microaggregate (MI), and silt plus clay (SC) at top (TSL) and sub-surface (SSL) soil layers in semi-arid restored land.

	TSL											
	BS			MA			MI			SC		
	HI	Aromaticity	DDI	HI	Aromaticity	DDI	HI	Aromaticity	DDI	HI	Aromaticity	DDI
C.cil[#]	0.891a[$]	0.292a	0.335d	1.847a	1.095a	0.635d	1.605a	1.327a	0.828b	2.194a	1.646a	0.524c
P.max	0.478c	0.305a	0.634c	1.428b	1.096a	0.768c	1.238b	1.328a	1.074a	1.456c	1.147bc	0.789b
C.ful	0.415d	0.314a	0.745b	1.347b	1.107a	0.825b	1.166b	1.341a	1.154a	1.326c	1.259b	0.877a
H.con	0.802b	0.302a	0.381d	1.765a	1.110a	0.629d	1.533a	1.344a	0.877b	2.054b	1.621a	0.566c
S.ner	0.904a	0.286a	0.325d	1.862a	1.082a	0.585e	1.618a	1.310a	0.815b	2.212a	1.532a	0.515c
V.ziz	0.457c	0.314a	0.682c	1.410b	1.111a	0.792c	1.222b	1.346a	1.107a	1.406c	1.064c	0.831a
URC	0.284e	0.261b	0.842a	1.125c	1.111a	1.095a	1.023c	0.954b	0.856b	1.015d	0.984d	0.760b
	SSL											
C.cil	0.894b	0.275a	0.149c	1.850a	1.060a	0.573d	1.608a	1.284a	0.799b	2.198a	1.609a	0.505c
P.max	0.472c	0.305a	0.215b	1.419b	1.095a	0.772c	1.230b	1.327a	1.079a	1.447b	1.147b	0.793b
C.ful	0.418c	0.309a	0.229b	1.351b	1.097a	0.813b	1.170b	1.330a	1.137a	1.329b	1.049c	0.865a
H.con	0.899b	0.301a	0.162c	1.856a	1.112a	0.599d	1.613a	1.347a	0.836b	2.204a	1.614a	0.529c
S.ner	0.935a	0.295a	0.156c	1.894a	1.102a	0.583d	1.646a	1.336a	0.812b	2.250a	1.542a	0.514c
V.ziz	0.451c	0.309a	0.221b	1.400b	1.101a	0.788c	1.213b	1.334a	1.102a	1.396b	1.053c	0.827a
URC	0.291d	0.268b	0.850a	1.141c	1.127a	1.095a	1.037c	0.967b	0.856b	1.029c	0.998d	0.760b

[#]*See materials and methods for details*

[$]*Statistical inference according to Tukey's test is shown by lowercase letters.*

Table 5 Correlations of temperature sensitivity of labile and recalcitrant C (Q_{10L} and Q_{10R}) with quality parameters (humification index: HI; aromaticity; and degree of decomposition: DDI) of soil organic matter, concentration of labile and recalcitrant C (C_L and C_R), and root litter carbon quality in bulk soils (BS), macroaggregate (MA), microaggregate (MI), and silt plus clay (SC) at top (TSL) and sub-surface (SSL) soil layers in semi-arid restored land.

		Soil carbon quality			Root litter carbon quality				Soil carbon quantity	
TSL		HI	DDI	Aromaticity	Carboxylate	Polysaccharide	Aromatic+Phenolic	Aliphatic	C_L	C_R
BS	Q_{10L}	-0.287 ^{ns}	-0.187 ^{ns}	-0.833	0.834	0.659	-0.150 ^{ns}	-0.476 ^{ns}	0.800	-0.100 ^{ns}
	Q_{10R}	0.769	0.771	0.804	0.456 ^{ns}	-0.029 ^{ns}	0.657	0.400 ^{ns}	0.511 ^{ns}	0.751
MA	Q_{10L}	-0.326 ^{ns}	-0.374 ^{ns}	-0.634	0.787	0.651	-0.311 ^{ns}	-0.485 ^{ns}	0.490 ^{ns}	-0.098 ^{ns}
	Q_{10R}	0.758	0.782	0.799	-0.446 ^{ns}	0.098 ^{ns}	0.633	-0.614 ^{ns}	-0.113 ^{ns}	0.894
MI	Q_{10L}	-0.009 ^{ns}	-0.339 ^{ns}	-6.471	0.706	0.833	-0.141 ^{ns}	-0.513 ^{ns}	-0.300 ^{ns}	0.094 ^{ns}
	Q_{10R}	0.845	0.856	0.745	-0.512 ^{ns}	0.089 ^{ns}	0.661	0.323 ^{ns}	-0.359 ^{ns}	0.868
SC	Q_{10L}	-0.097 ^{ns}	-0.128 ^{ns}	0.079 ^{ns}	-0.332 ^{ns}	-0.198 ^{ns}	-0.290 ^{ns}	0.694	0.644	-0.074 ^{ns}
	Q_{10R}	0.827	0.783	0.213 ^{ns}	-0.607 ^{ns}	-0.110 ^{ns}	0.662	-0.681	-0.464 ^{ns}	0.827
SSL		HI	DDI	Aromaticity	Carboxylate	Polysaccharide	Aromatic+Phenolic	Aliphatic	C_L	C_R
BS	Q_{10L}	-0.463 ^{ns}	-0.474 ^{ns}	-0.636	-0.351 ^{ns}	0.269 ^{ns}	-0.326 ^{ns}	-0.406 ^{ns}	0.768	-0.198 ^{ns}
	Q_{10R}	0.659	0.686	0.719	-0.436 ^{ns}	0.503 ^{ns}	-0.427 ^{ns}	-0.428 ^{ns}	-0.208 ^{ns}	0.721
MA	Q_{10L}	-0.301 ^{ns}	-0.291 ^{ns}	-0.635	-0.252 ^{ns}	0.124 ^{ns}	-0.119 ^{ns}	-0.424 ^{ns}	0.679	-0.380 ^{ns}
	Q_{10R}	0.819	0.837	0.738	0.187 ^{ns}	0.151 ^{ns}	0.428 ^{ns}	-0.178 ^{ns}	-0.009 ^{ns}	0.730
MI	Q_{10L}	-0.262 ^{ns}	-0.261 ^{ns}	-0.731	-0.425 ^{ns}	0.491 ^{ns}	-0.485 ^{ns}	-0.331 ^{ns}	0.637	-0.277 ^{ns}
	Q_{10R}	0.890	0.891	0.737	-0.214 ^{ns}	-0.061 ^{ns}	-0.049 ^{ns}	-0.362 ^{ns}	-0.189 ^{ns}	0.734
SC	Q_{10L}	0.234 ^{ns}	0.233 ^{ns}	0.238 ^{ns}	0.431 ^{ns}	0.523 ^{ns}	0.338 ^{ns}	0.480 ^{ns}	0.685	0.197 ^{ns}
	Q_{10R}	0.976	0.764	0.131 ^{ns}	-0.357 ^{ns}	0.118 ^{ns}	-0.215 ^{ns}	-0.485 ^{ns}	-0.050 ^{ns}	0.820

Green and red coloured cell indicated significant positive and negative corelations at $p \leq 0.05$, respectively; ns: non-significant relations at $p \leq 0.05$.

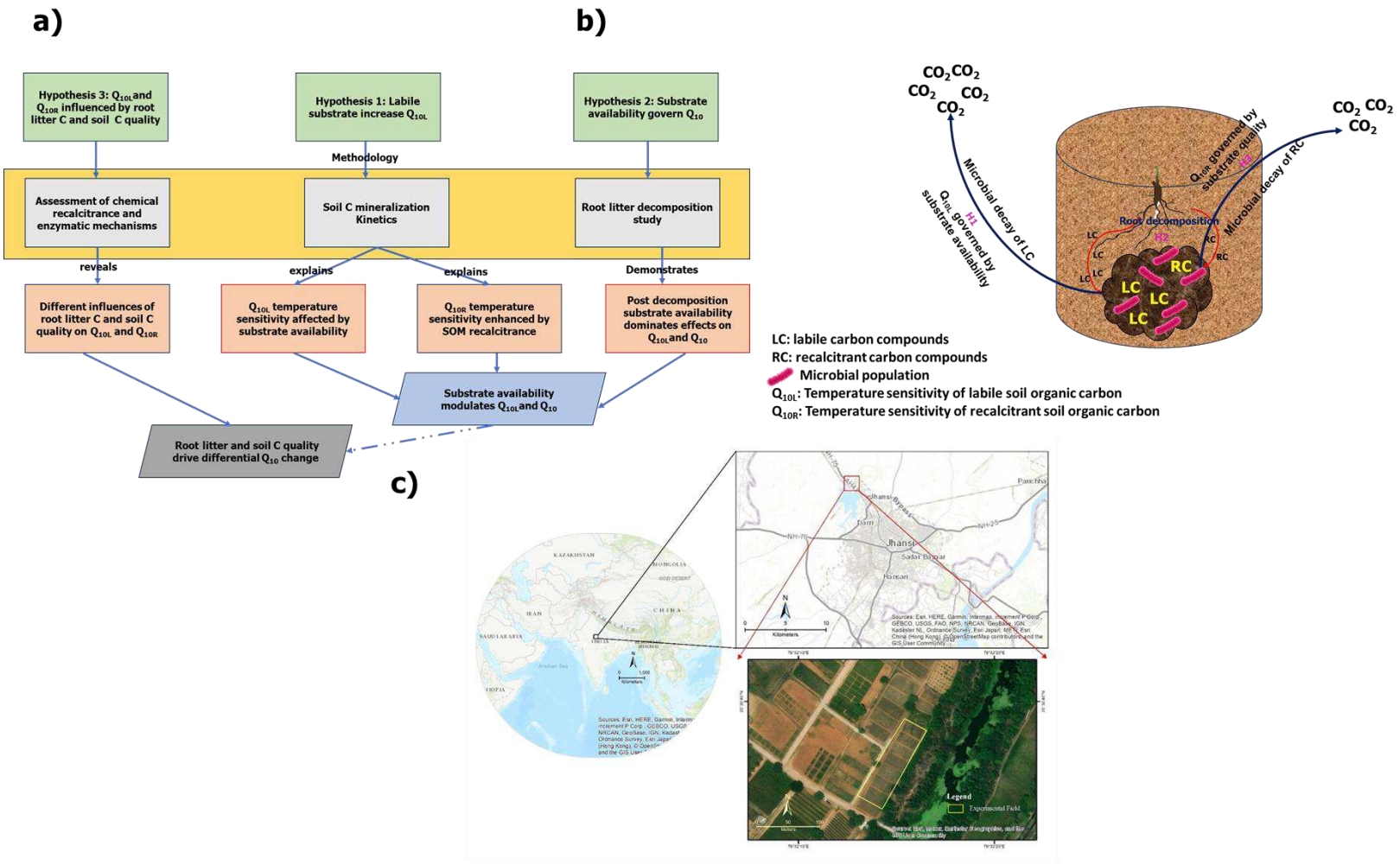

Figure 1: a) Schematic representation of three hypotheses b) Pictorial display of the hypotheses; c) The geographic location of the experimental site and lay out of experiment.

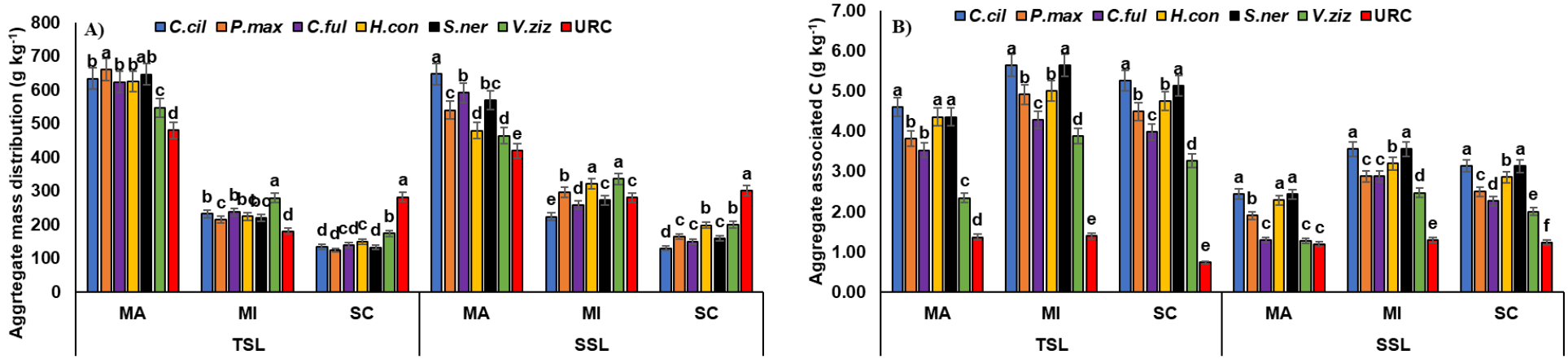

Figure 2. Impact of grass covers on A) soil aggregate mass distribution and B) aggregate associated soil organic carbon (C) concentration at top (TSL) and sub-surface (SSL) soil layers in semi-arid restored land. Error bars signify standard error of mean. The columns with same lowercase letters within an aggregate size fraction are not statistically different following Tukey's HSD test.;

MA: Macroaggregates; MI: Microaggregates: SC: silt plus clay.

C.cil: *Cenchrus ciliaris*; C.ful: *Chrysopogon fulvus*; P.max*: Panicum maximus;* S.ner*: Sehima nervosum*; H.con*: Heteropogon contortus*; V.ziz*: Vetiveria zizanioides*; URC: Unrestored control;

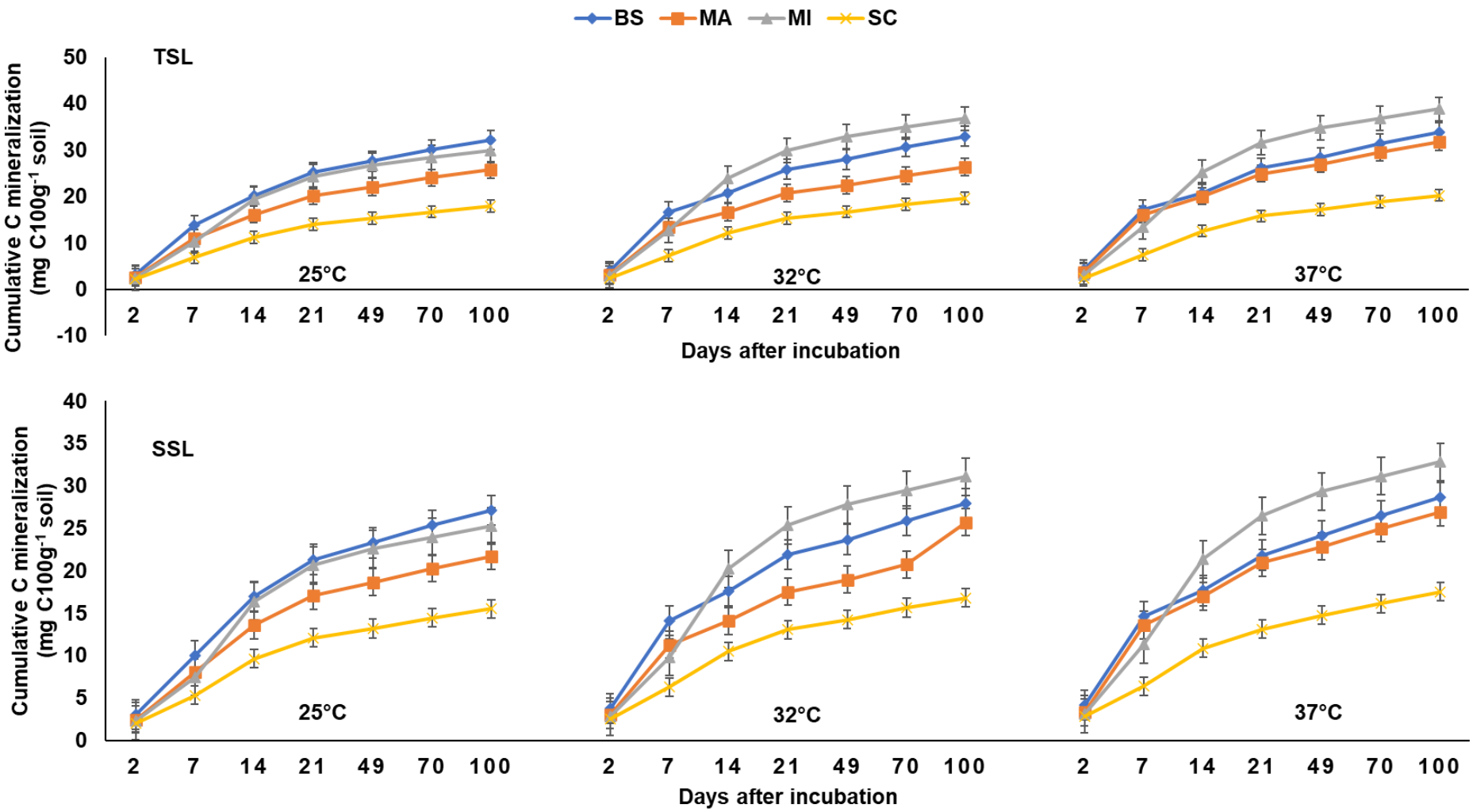

911

912 Figure 3. Impact of incubation temperatures (at 25, 32, and 37 °C) on cumulative carbon (C) mineralization from bulk soil (BS), macroaggregate (MA),
913 microaggregate (MI), and silt plus clay (SC) temperatures at top (TSL) and sub-surface (SSL) soil layers in semi-arid restored land. Error bars signify
914 statistical difference following Tukey's HSD test.

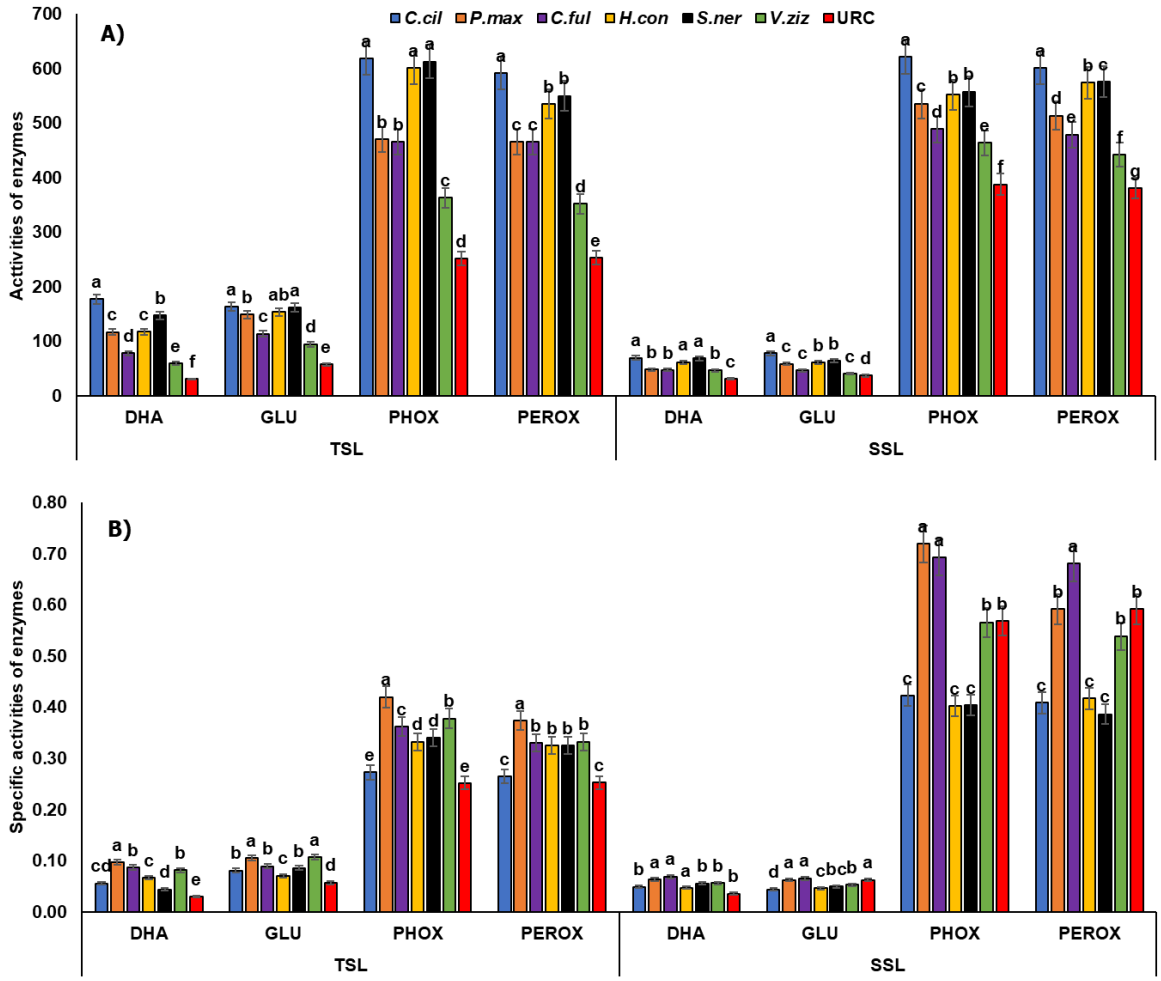

Figure 4. Impact of grass covers on A) absolute activities and B) specific activities dehydrogenase (DHA; µg TPF g^{-1} $24h^{-1}$), β-glucosidase (GLU; µg PNG g^{-1} $2h^{-1}$), phenoloxidase (PHOX; µg ABTS g^{-1} h^{-1}), and peroxidase (PEROX; µg ABTS g^{-1} h^{-1}) activities at top (TSL) and sub-surface (SSL) soil layers in semi-arid restored land. Error bars signify standard error of mean. The columns with same lowercase letters within an aggregate size fraction are not statistically different following Tukey's HSD test.

C.cil: *Cenchrus ciliaris*; C.ful: *Chrysopogon fulvus*; P.max*: Panicum maximus;* S.ner*: Sehima nervosum*; H.con*: Heteropogon contortus*; V.ziz*: Vetiveria zizanioides*; URC: Unrestored control

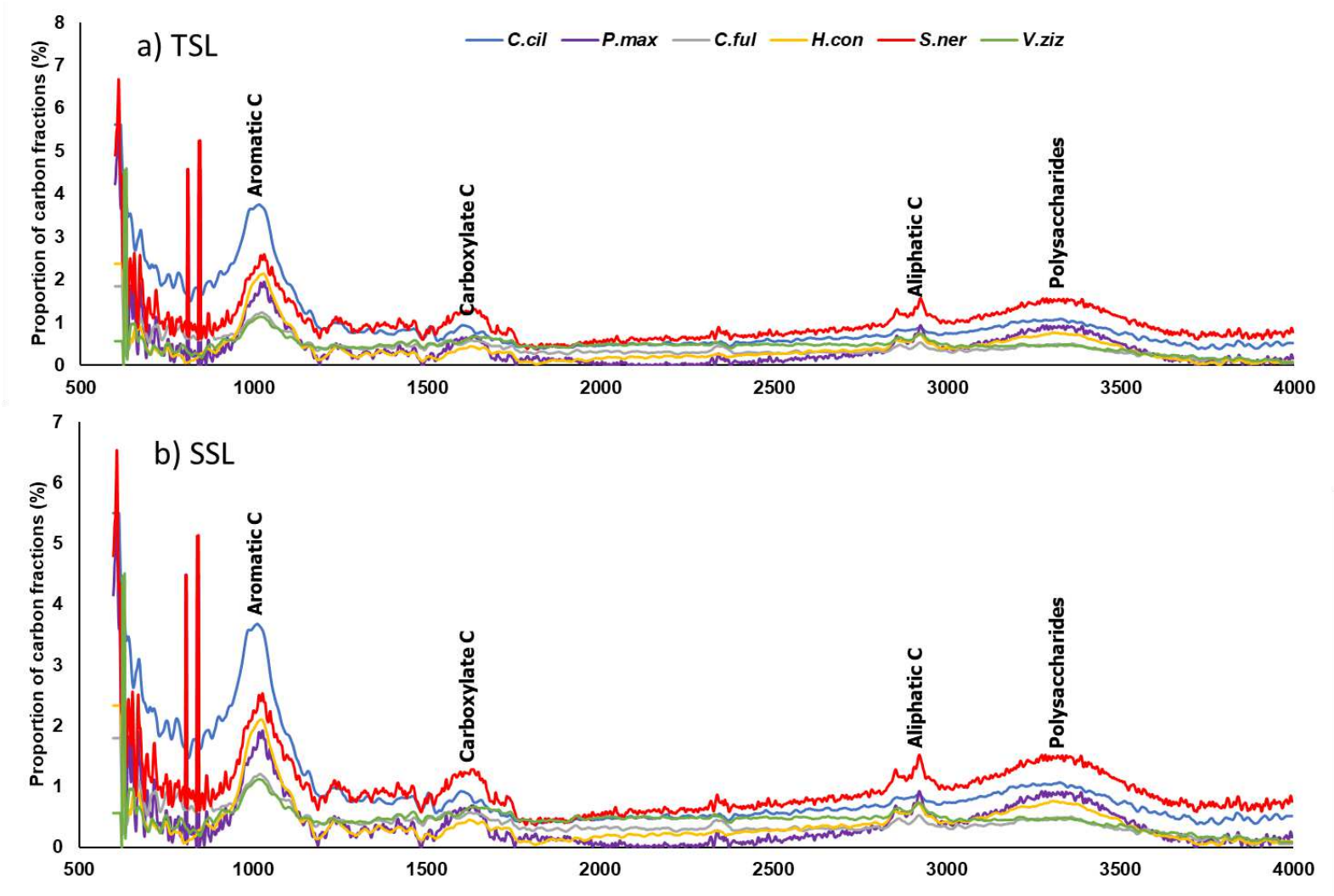

927

928 Figure 5. The proportions of different organic C fractions in root litters of different grasses at A) top (TSL) and B) sub-surface (SSL) soil layers
929 in semi-arid restored land.

930 C.cil: *Cenchrus ciliaris*; C.ful: *Chrysopogon fulvus*; P.max*.: Panicum maximus;* S.ner*.: Sehima nervosum*; H.con*.: Heteropogon contortus*; V.ziz*.: Vetiveria zizanioides*;

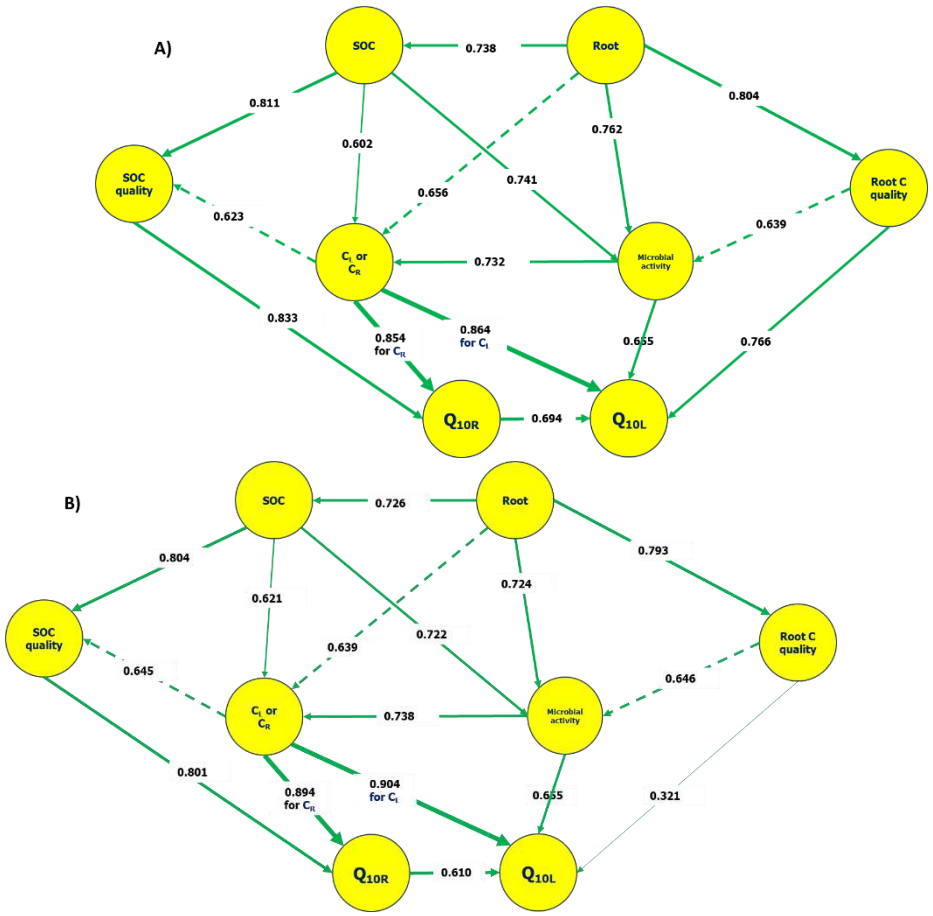

Figure 6. Path analysis depicting impact of labile and recalcitrant C pools (C_L and C_R), soil organic matter quality, and root litter C quality on temperature sensitivity of labile and recalcitrant C pools (Q_{10L} and Q_{10R}) at A) top and B) sub-surface soil layers. Models satisfactorily fitted to data based on $\chi 2$ and RMSEA analyses [$\chi 2 = 112.56$, GFI= 0.69, RMSEA < 0.001]. Widths of the arrows indicate the strength of the casual relationship. Dashed arrows represent indirect effects, solid arrows indicate direct relationships.

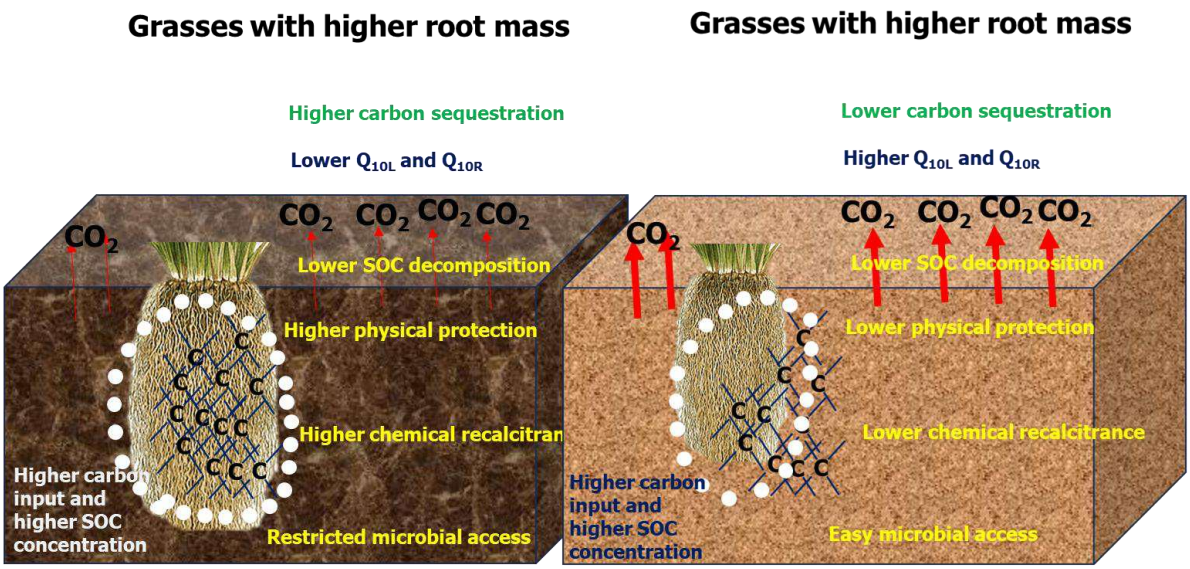

942

943 Figure 7. Schematic representation of roles of root litter traits on temperature sensitivity (Q_{10})
944 and soil carbon sequestration.

Supplementary Files

This is a list of supplementary files associated with this preprint. Click to download.

- Supplementary040425.docx